Mitochondrial maintenance under oxidative stress depends on mitochondrial but not nuclear α isoform of OGG1

Running title: Role of α-OGG1 in human mitochondria

Debora Lia[1,2,3], Aurelio Reyes[4], Julliane Tamara Araújo de Melo[1,5], Tristan Piolot[6], Jan Baijer[1,2,3], Juan Pablo Radicella[1,2,3], Anna Campalans[1,2,3]

[1] Institut de biologie François Jacob (IBFJ). Institute of Cellular and Molecular Radiobiology, CEA, UMR967 INSERM, F-96265 Fontenay aux Roses, France

[2] Université Paris Diderot, France

[3] Université Paris-Sud, France

[4] MRC Mitochondrial Biology Unit. University of Cambridge. Cambridge CB2 0XY. United Kingdom

[5] Laboratório de Biologia Molecular e Genômica, Departamento de Biologia Celular e Genética, Centro de Biociências, Universidade Federal do Rio Grande do Norte, Natal, RN, Brazil

[6] Institut Curie, CNRS UMR3215, INSERM U934, 75248, Paris, France / Present address: UMR7241 CNRS, INSERM, College-de-France, 75005, Paris, France

Correspondence to anna.campalans@cea.fr. ORCID iD 0000-0001-7089-6891

Key words (3-6): mitochondria, DNA repair, 8-oxoG, OGG1

Summary statement

α-OGG1 is imported into mitochondria where its glycosylase activity is essential for mitochondrial maintenance in human cells exposed to oxidative stress.

Abstract

Accumulation of 8-oxoG in mtDNA and mitochondrial dysfunction have been observed in cells deficient for the DNA glycosylase OGG1 exposed to oxidative stress. In human cells up to eight mRNAs for OGG1 have been described as generated by alternative splicing and it is still unclear which of them ensures the repair of 8oxoG in human mitochondria. Here, we show that the α-OGG1 isoform, considered up to now to be exclusively localized in the nucleus, has a functional mitochondrial targeting signal and is imported into the mitochondria. We analyzed the submitochondrial localization of α-OGG1 with unprecedented resolution and we show that the glycosylase is associated with DNA in nucleoids. This association does not depend on the cell cycle or the replication of mtDNA. Using α-OGG1 deficient human cells, we show that the presence of α-OGG1 inside mitochondria and its enzymatic activity are required to preserve mitochondrial network in cells exposed to oxidative stress. Altogether, these results evidence a new role of α-OGG1 in the mitochondria and indicate that the same isoform ensures the repair of 8oxoG in both nuclear and mitochondrial genomes and that its activity in mitochondria is sufficient for the recovery of the organelle function after oxidative stress.

Introduction

The mammalian mitochondrial genome consists of a circular double-stranded DNA molecule of approximately 16 kb in length and accounts for 1% to 2% of the total DNA in the cell. It encodes for only 13 proteins, all of them involved in oxidative phosphorylation and ATP synthesis, as well as for two rRNAs (12S rRNA and 16S rRNA) and 22 tRNAs that are required for mitochondrial protein synthesis. However, up to 1500 proteins encoded by the nuclear genome are found inside mitochondria, including proteins required for replication, transcription and repair of mitochondrial DNA (mtDNA). mtDNA is highly packed in DNA-protein assemblies constituting the mitochondrial nucleoids, that can be clearly observed by fluorescence microscopy as discrete foci distributed throughout the mitochondrial network (Alam et al., 2003; Legros et al., 2004). Nucleoids are anchored to the mitochondrial inner membrane and are composed of one or two DNA molecules (Kukat *et al*, 2011) and several core proteins involved in DNA packaging, transcription and signaling. In particular, TFAM (Mitochondrial Transcription Factor A), a key activator of mitochondrial transcription as well as a participant in mitochondrial genome replication, is a major component of the nucleoid and is required for the mtDNA packaging. Besides the core proteins, many other proteins transiently associate with mitochondrial nucleoids (Gilkerson *et al*, 2013).

Even though many proteins known for their role in nuclear DNA repair (BER, mismatch repair, single and double strand break repair) are imported into mitochondria (Kazak *et al*, 2012), what mechanisms participate in the maintenance of mtDNA is still an open question. Mitochondrial biogenesis and dynamics, including degradation of damaged mitochondria by mitophagy, also play essential roles in preserving the stability of the mitochondrial genome. The scenario becomes even more complex if we take into consideration that each cell contains a large number of mtDNA molecules, up to several thousands, depending on the cell type. Thanks to cycles of fusion and fission that promote mixing and homogenization of mitochondrial contents, cells maintain a certain level of heteroplasmy in which mutant and wt mtDNA molecules coexist (Mishra & Chan, 2014). For most of the mtDNA mutations described so far, no phenotypic alteration is detectable unless mutant mtDNA molecules exceed 60% of the total mtDNA (Gilkerson et al., 2008, Schon and Gilkerson, 2010). Considering that accumulation of mutations or deletions and the loss of mtDNA are involved in many different human diseases, a better understanding of the cellular processes involved in the maintenance of this molecule is of major importance.

Oxidative mtDNA damage has been reported to be more extensive and persistent than nuclear DNA damage (Yakes and Van Houten, 1997; Richter et al., 1988). It has been proposed that this higher sensitivity of mtDNA could be due to the absence of histones in mitochondria, facilitating the access of ROS to mtDNA. However, this idea is not supported by the tight packaging of mtDNA around the TFAM protein in nucleoids resulting in a highly compacted structure. Accumulation of mtDNA damage could also be due to the proximity of the mtDNA to the continuous ROS production by the mitochondrial electron transport chain. Persistence of oxidative damage in mtDNA could lead to the accumulation of deletions or mutations at the origin of mitochondrial dysfunction (Shigenaga et al., 1994). Mitochondrial DNA damage has been linked to

loss of mitochondrial membrane potential, increased reactive oxygen species (ROS) generation and cell death (Santos et al., 2003).

One of the most frequent DNA alterations induced by ROS is 8-oxoG, a product of oxidation of guanine. Several lines of evidence suggest that accumulation of 8-oxoG in mtDNA contributes to the mitochondrial dysfunction observed during aging and in neurodegenerative disorders (Druzhyna et al., 2008). Three enzymes are involved in the avoidance of the accumulation of 8-oxoG and its mutagenic consequences. MTH1 detoxifies the pool of nucleotides by hydrolyzing the 8-oxo-2′-deoxyguanosine triphosphate (8-oxo-dGTP) to 8-oxo-dGMP, the DNA glycosylase OGG1 excises 8-oxoG paired with cytosine in DNA, and MUTYH (MYH), another DNA glycosylase, removes the Adenine paired to the 8-oxoG after replication, thus giving another opportunity to OGG1 for removing the 8-oxoG (Oka et al., 2014). These three enzymes are mostly known for their role in the nucleus but they are also targeted to mitochondria and their deficiency causes mtDNA loss and results in mitochondrial dysfunction. Indeed, *Ogg1* knock-out mice accumulate high levels of 8-oxoG in mitochondria (Souza-Pinto et al., 2001). It has also been shown that MTH1 and OGG1 play essential roles in the protection of mtDNA during neurogenesis, and that *Mth1/ Ogg1* double knock-out mice accumulate 8-oxoG and display reduced mitochondrial membrane potential (Leon et al., 2016). Moreover, exposure of OGG1-deficient cells to oxidative stress results in mitochondrial dysfunction, with reduction of mtDNA levels, decrease of mitochondrial membrane potential, increase of mitochondrial fragmentation and reduced levels of proteins encoded by mtDNA, possibly linked to accumulation of oxidative mtDNA damage (Wang et al., 2011).

OGG1 initiates the Base Excision Repair (BER) pathway by specifically recognising and excising 8-oxoG. In mitochondria, OGG1 DNA glycosylase activity is thought to be followed by that of other BER proteins: AP endonuclease APE1, DNA polymerase Pol-gamma and DNA Ligase III. All these BER proteins are encoded by the nuclear genome and are imported into the mitochondria (Kazak *et al*, 2012). Pol-gamma and Ligase III are not only involved in BER but are essential for mtDNA replication, and defects in those proteins result in mtDNA instability leading to dramatic mitochondrial and cellular dysfunctions (Simsek et al., 2011; Trifunovic et al., 2004; Zhang et al., 2011). While for many years, Pol-gamma has been considered to be the only polymerase present inside mitochondria, recent reports have shown the presence of Pol-beta inside the organelle (Sykora et al., 2017). These findings indicate that from the recognition of the lesion to the ligation step, the very same BER enzymes act in both the nucleus and the mitochondria to ensure the repair of oxidative DNA damage. According to the information present in the National Center for Biotechnology Information (NCBI) many different *OGG1* mRNAs (and potentially proteins) can be generated from the *OGG1* gene by alternative splicing in human cells (Takao, 1998; Nishioka et al., 1999; Ogawa et al., 2014; Furihata et al., 2016). Experimental evidence is still lacking concerning which isoforms are indeed translated in the cell. All potential isoforms (OGG1-1a, −1b, −1c, −2a, −2b, −2c, −2d and −2e) share the same N-terminal domain containing a Mitochondrial Targeting Sequence (MTS). The OGG1-1a (also named α-OGG1) is the only isoform to have also a Nuclear Localization Signal (NLS) and has therefore been

defined as the nuclear isoform of OGG1. Which of the OGG1 isoforms is responsible for the repair of the 8-oxoG in mtDNA is still unclear. Despite the very high conservation of the DNA glycosylases between mouse and human, to date, only the isoform corresponding to the human α-OGG1 has been identified in mouse and therefore proposed to ensure the 8-oxoG glycosylase activity in both nucleus and mitochondria. The artificial targeting of human α-OGG1 to mitochondria, by a fusion to the MTS of MnSOD allows the complementation of mitochondrial dysfunction observed in OGG1 deficient cells, suggesting that this isoform can also be active in mitochondria and efficient in the removal of 8-oxoG (Dobson et al., 2000; Rachek, 2002).

In this study, using a combination of biochemical and imaging techniques, we show that α-OGG1 is normally imported into mitochondria and that both the MTS and the NLS signals are functional and sufficient to determine the subcellular localization of the enzyme. In agreement with the function of the protein in DNA repair, we describe the association of α-OGG1 with mtDNA in the mitochondrial nucleoids independently of the cell cycle phase and the mitochondrial DNA replication status. Furthermore, our results show that the presence and glycosylase activity of α-OGG1 inside mitochondria are essential to preserve mitochondrial function in human cells exposed to oxidative stress.

Results

α-OGG1 is imported into mitochondria where it associates with the inner mitochondrial membrane

Using a monoclonal antibody that specifically recognizes an epitope only present in the α-OGG1 isoform, we showed that this isoform was present in both nuclear and mitochondrial protein fractions (Fig. 1A). Likewise, a α-OGG1 tagged with the FLAG epitope was produced and an anti-FLAG antibodies was used to study the subcellular localization of the fusion protein. As for the endogenous protein, α-OGG1-FLAG was present in both nuclear and mitochondrial fraction (Fig. 1B). U2OS cells expressing α-OGG1-FLAG were stained with Mitotracker Red prior to fixation and immunostained with an anti-FLAG antibody. As shown in Fig.1C, α-OGG1-FLAG protein was present in both the nucleus and the mitochondria (Fig. 1C).

To determine α-OGG1 sub-mitochondrial localization, we performed protease digestion assays on isolated mitochondria. Mitochondria from U2OS cells were treated with increasing amounts of Proteinase K to degrade mitochondrial proteins facing cytoplasm. α-OGG1 was protected from proteinase K digestion indicating that the protein was located inside the mitochondria (Fig1D). To better define the localization of α-OGG1, sucrose-gradient purified mitochondria from HEK-293 cells were treated with hypotonic buffer or digitonin to disrupt the outer mitochondrial membrane and allow trypsin to degrade proteins from both the outer membrane and the intermembrane space. Proteins that localize in the outer mitochondrial membrane like TOM20 are fully degraded whenever trypsin is added, even in intact mitochondria. TIM23 is localized in the inner mitochondrial membrane with a domain protruding the intermembrane space that is cleaved when the outer membrane is disrupted in hypotonic or digitonin treatments. Proteins from the mitochondrial matrix like ETFB and the inner membrane facing the matrix like SDHA are not digested neither in hypotonic nor in

digitonin treatments and same results were obtained for α-OGG1 indicating that at least a fraction of the protein was either localized in the inner mitochondrial membrane or in the mitochondrial matrix (Fig. 1E). Finally, association of α-OGG1 with mitochondrial membranes was studied by treating purified mitochondria with low or high salt concentrations. α-OGG1 remained insoluble even at high salt concentrations (Fig. 1F). Altogether, these results show that α-OGG1 is located both in the nucleus and in the mitochondria where it associates with the inner mitochondrial membrane.

α-OGG1 is associated with mtDNA in nucleoids

Confocal microscopy showed that α-OGG1-Flag was not homogeneously distributed inside mitochondria but accumulated at punctate foci that resembled the mitochondrial nucleoids. To determine if α-OGG1 was actually a nucleoid-associated protein, co-localisation of α-OGG1-FLAG with nucleoid markers, was investigated. Co-localization between α-OGG1 and mtDNA and TFAM was observed (Fig. 2A, B) with Pearson correlation coefficients of 0.75 and 0.8, respectively. The spatial organization of α-OGG1 and TFAM in mitochondrial nucleoids was further explored by using Structured Illumination Microscopy (3D-SIM). This approach revealed that α-OGG1 was clearly surrounding TFAM, a marker for the nucleoid core (Fig. 2C, D). The association of α-OGG1 with mitochondrial nucleoids was further confirmed by fractionation on an iodixanol gradient of detergent-solubilized mitochondria from HEK 293T cells. Southern and Western blot analysis of the gradient fractions revealed that a significant amount of α-OGG1 co-fractionated with mtDNA in the same way the mtDNA binding protein TFAM did (Fig. 2E, fractions 9-11 with a peak in 9) while proteins not binding to mtDNA like GARS did not show this co-fractionation. Collectively, these results indicate that α-OGG1 associates with mtDNA in the nucleoids.

α-OGG1 contains functional nuclear and mitochondrial targeting signals

In agreement with the presence of α-OGG1 in both nuclear and mitochondrial compartments, several softwares for the prediction of targeting signals determine a very strong probability for α-OGG1 to be imported into mitochondria and identify a canonical Mitochondrial Targeting Sequence (MTS) at the N-terminus of the protein. Interestingly, a second in frame AUG codon was found at the N-terminal part of the *OGG1* messenger and shown to be highly conserved among mammals (Fig. 3A and Fig. S1). Intriguingly, an initiation of translation at the second AUG would result in a protein with a truncated MTS and thus would have a reduced probability to be localized inside mitochondria (Fig. 3B). Finally, a TOM20 recognition motif (RKYF) in position 97-100 of α-OGG1, suggested that α-OGG1 can be imported into the mitochondria by the TIM/TOM pathway (Schulz et al., 2015; Model et al., 2008).

To define the role of the MTS and NLS targeting signals, we expressed full length α-OGG1 or truncated versions, lacking either the MTS or the NLS, fused to the FLAG epitope and analyzed their subcellular localization (Fig. 3C). While, as mentioned above, the full length α-OGG1 was present in both mitochondrial and nuclear compartments, disruption of the MTS (OGG1-ΔMTS), due to the initiation of

translation at the second in frame AUG, resulted in a protein localized exclusively in the nucleus. Interestingly, substitution of the glycine in position 12 by a glutamic acid, a mutation identified in kidney cancer cells (Audebert et al, 2002), also impaired the mitochondrial import of the protein (Fig 3C). Deletion of the NLS gave rise to a protein mostly localized in the mitochondria (Fig. 3D, E). Taken together, these results indicate that mitochondrial and nuclear targeting sequences co-exist in α-OGG1 and that both signals are functional and can determine the subcellular localization of the enzyme.

Import of α-OGG1 to mitochondria is independent of the cell cycle or mtDNA replication

As mitochondrial import has been shown to be modulated through the cell cycle (Harbauer et al., 2014), we decided to explore if the subcellular distribution of α-OGG1 was cell cycle-dependent. The incorporation of EdU was used to identify cells in S phase and an antibody against the kinetochore protein CENP-F was used for cells in G2 phase. Cells in G1 are negative for both EdU and CENP-F. As shown in Fig. 4A, OGG1(WT)-Flag was detected in mitochondria independently of the cell cycle phase and the proportion of cells with mitochondrial staining remained unchanged throughout the cell cycle. We further investigated whether the mtDNA replication status influenced the sub-organelle localization of α-OGG1, as it is the case for several proteins involved in mtDNA maintenance (Rajala et al., 2014). EdU incorporation was used to visualize the mitochondrial nucleoids undergoing replication on transiently double transfected cells expressing α-OGG1(WT)-Flag and MTS-Turquoise2. An antibody against TFAM was used to label mitochondrial nucleoids (Fig. 4C, D). More than 500 nucleoids were analyzed to determine their replication state and the presence or absence of the glycosylase. As can be appreciated in Fig. 4C, α-OGG1-FLAG could be detected in both EdU positive and negative nucleoids, clearly indicating that the association of the glycosylase with the nucleoids is not dependent on DNA replication. Altogether these results show that the mitochondrial import of α-OGG1 and its association to mtDNA is not dependent on the cell cycle phase or on mtDNA replication status.

OGG1-deficiency is associated with mitochondrial dysfunction after an oxidative stress

Considering that the only known activity for OGG1 is the repair of 8-oxoG, we next studied the impact of OGG1 deficiency in the response of mitochondria to menadione-induced oxidative stress that results in the induction of 8-oxoG in mtDNA (Oka et al., 2008). Transfection of U2OS cells with OGG1 directed siRNA resulted in more than 90% decrease of both transcript and protein levels of α-OGG1 72 h after transfection (Fig. 5A). Cells transfected with siRNA against OGG1 or control siRNA were exposed to menadione and mitochondrial parameters were evaluated. After menadione treatment, we found a higher increase in mitochondrial superoxide production in OGG1-deficient cells when compared to controls (Fig. 5B,C). In addition, the use of TMRE probe to monitor mitochondrial membrane potential revealed that menadione treatment induced a higher loss of mitochondrial membrane potential in OGG1 silenced cells, while no difference was observed between the two cell populations in basal conditions (Fig. 5D, E). The

loss of mitochondrial activity observed was not due to a loss in mitochondrial mass as MitoTracker Green staining was not affected by the treatment.

To monitor single cell responses over time, we performed real time microscopy. Cells transfected with a siRNA against OGG1 or with a control siRNA, were treated with 50 μM of menadione for one hour, washed and imaged for 2 hours at a frame rate of one image every two minutes. Most of the mitochondria from cells transfected with a control siRNA showed a stable TMRE staining over time after menadione treatment, indicating the maintenance of a positive membrane potential. In contrast, approximately 40% of OGG1-deficient cells showed a progressive and fast loss of membrane potential leading to the inactivation of the entire mitochondrial network (Fig. 5F). These results revealed that human OGG1 deficient cells show a mitochondrial dysfunction when exposed to oxidative stress, with a major production of mitochondrial superoxide and loss of mitochondrial membrane potential.

α-OGG1 mitochondrial localization and enzymatic activity are required to prevent mitochondrial dysfunction in cells exposed to oxidative stress.

To determine if α-OGG1 could rescue the mitochondrial defects observed in OGG1 deficient cells, we established U2OS cell lines stably expressing α-OGG1(WT)-Flag or the exclusively nuclear α-OGG1(ΔMTS)-Flag. The deletion of 10 aminoacids at the N-terminus of OGG1 didn't affect the enzymatic activity of the enzyme, as expression of α-OGG1(ΔMTS)-FLAG resulted in the same level of 8-oxoG DNA glycosylase activity in total cell extracts than that of extracts from cells expressing the full-length protein (Fig. 6A). In order to specifically reduce the levels of the endogenous OGG1, silent mutations were introduced in the sequence of the ectopically expressed proteins to make them resistant to the siRNA against OGG1 (Fig. 6B).

Wild-type U2OS cells or cells stably overexpressing the different isoforms of the protein were transfected with the siRNA against OGG1. Three days after transfection, the cells were stained with TMRE or MitoSOX, treated with menadione, and analyzed. The oxidative stress induced a significantly higher mitochondrial ROS production along with higher loss of mitochondrial membrane potential in OGG1 deficient cells compared to cells transfected with the control siRNAs. Both parameters were rescued by expression of a WT version of α-OGG1 but not by the expression of the mutant isoform (Fig. 6C,D), indicating that the presence of the α-OGG1 DNA glycosylase in the mitochondria is required for the recovery of the organelle from the oxidative stress.

Prominent fragmentation of the mitochondrial network was observed in U2OS cells after exposure to menadione. This fragmentation was characterized by a rapid transition from a filamentous and branched network to a fragmented one, with isolated, round-shaped mitochondria (Fig. 7A). To evaluate if overexpression of α-OGG1 in mitochondria could suppress the fragmentation of this organelle after menadione treatment, U2OS cells were transiently transfected with constructs expressing α-OGG1(WT)-

FLAG, α-OGG1(ΔMTS)-FLAG or the catalytically inactive mutant α-OGG1(K249Q)-FLAG (Fig. 7A). The latter mutant displayed the same subcellular distribution as the WT protein, and was localized both in the nucleus and in mitochondria (Fig. S2). The percentage of cells with a preserved mitochondrial network was quantified in basal conditions and after exposure to oxidative stress (Fig. 7B). Only the overexpression of the α-OGG1(WT)-FLAG protein resulted in a normal mitochondrial network in cells exposed to menadione. Further analysis of mitochondrial morphology parameters on binarized images corroborated that after menadione treatment mitochondrial length and degree of branching were comparable in non-transfected and α-OGG1(ΔMTS)-FLAG or α-OGG1(K249Q)-FLAG overexpressing cells, while in α-OGG1(WT)-FLAG overexpressing cells the network was better preserved (Fig.7C,D).

Taken together, these results indicate that mitochondrial α-OGG1 is essential to preserve mitochondrial morphology and function after exogenous oxidative stress. In addition, because the catalytically inactive mutant α-OGG1(K249Q)-FLAG displays the same subcellular localization than the WT enzyme and co-localizes with mitochondrial nucleoids, our data strongly suggest that the DNA glycosylase activity and thus removal of 8-oxoG is required to protect mitochondrial physiology from oxidative stress.

Discussion

To be or not to be in the mitochondria

Despite clear evidence indicating the presence of a functional BER pathway inside human mitochondria, which isoform of the DNA glycosylase OGG1 is responsible for the recognition and excision of 8-oxoG in the mtDNA remained unclear. Although it was proposed that this activity could be performed by β-OGG1 (Oka et al., 2008), the lack of DNA glycosylase activity of this isoform renders its involvement in the repair of 8-oxoG unlikely (Hashiguchi et al., 2005). It was recently reported that in vitro purified OGG1 isoforms 1b and 1c present some enzymatic activity and could be responsible for the 8-oxoG removal from the mitochondrial genome (Furihata et al., 2015). However, there is no *in vivo* evidence for the existence of these OGG1 variants. It is not well known which transcripts are generated in different tissues and/or different physiological conditions and no experimental evidence determining which protein forms are indeed produced is available. In mouse, only a single transcript corresponding to the isoform α-OGG1 (OGG1-1a) has been identified and the protein has been shown to be functional in both nuclear and mitochondrial compartments. It is still unclear why so many *OGG1* transcripts are found in human cells. Because several of the potential polypeptides do not show any DNA glycosylase in vitro, they could have other, still non identified roles, or they might simply not be translated. Indeed, several global analyses comparing transcriptome and proteome data suggest that a large fraction of the reported mRNAs are never translated into proteins. Proteomic studies suggest that the vast majority of genes have a single dominant splice isoform that is the most highly conserved between different species (Tress et al., 2017). These

considerations would be in agreement with α-OGG1, the only OGG1 isoform conserved between mouse and human, being the 8-oxoG DNA glycosylase acting both, in the nucleus and in mitochondria, in both species.

Artificial targeting of human α-OGG1 to the mitochondria by the addition of the MnSOD MTS showed that the human protein can be active in this organelle and improve mitochondrial DNA repair and cellular survival in cells exposed to oxidative stress (Dobson et al., 2000; Rachek, 2002; Druzhyna et al., 2005; Kim et al., 2014). However, these experiments did not address the question of whether the endogenous α-OGG1 protein, without the additional targeting sequence, is imported inside the mitochondrial compartment. It was suggested that the MTS in α-OGG1 was not sufficient to target the protein to the mitochondria because of the presence of the very strong NLS at the C-terminus of the DNA glycosylase (Nishioka et al., 1999), despite the fact that the mouse protein, with a similarity close to 94% with α-OGG1 was found in both, the nucleus and the mitochondria. We showed here that isoform α-OGG1 is efficiently imported in mitochondria and that the MTS at the N-terminal part of the protein is functional and sufficient to ensure the targeting of the enzyme to the organelle. Consistently, several algorithms predict a canonical MTS for α-OGG1 and a mitochondrial localization of the protein with a very high probability, close to 90% (Fig. 3). In fact, the strength of the α-OGG1 MTS is not very different from that of the MnSOD MTS used in the chimeric MTS-OGG1 construct (Rachek et al., 2002) and our study definitely showed that the addition of an ectopic MTS is not required to ensure the efficient import of α-OGG1 into the mitochondria. The presence of dual targeting signals found in α-OGG1 is clearly not an exception as many proteins with dual functional signals for nuclear and mitochondrial localization have been identified (Yogev and Pines, 2011; Kazak et al., 2013).

Whether and how the subcellular localization of α-OGG1 is regulated remains an open question. In our experiments we did not observe any significant change in the subcellular distribution of α-OGG1 through the cell cycle or as a consequence of the exposure of the cells to oxidative stress. While most of the BER proteins are present in both the nucleus and the mitochondria, very little is known concerning the molecular mechanisms involved in the regulation of their subcellular localization. In the case of *Saccharomyces cerevisiae* DNA glycosylase Ntg1 the regulation of its subcellular distribution is modulated by oxidative stress and involves sumoylation (Griffiths et al., 2009; Swartzlander et al., 2010). The Ntg1 sumoylated sites have been recently identified and two of them are conserved in the human orthologue hNTH1, suggesting a similar regulation in higher eukaryotes (Swartzlander et al., 2016), although this possibility has not been further explored.

It is interesting to note that two in frame AUG codons are present in the N-terminal part of *OGG1* mRNA and that they are largely conserved among mammals (Fig. 3 and Fig. S1). As suggested by the prediction algorithms for mitochondrial targeting, our results clearly show that if translation is initiated at the second AUG, thus truncating the MTS, the resulting protein is exclusively localized into the nucleus. It has been clearly established that alternative start AUG codons within a single transcript largely contribute to the

diversity of the proteome (Van Damme et al., 2014), and in particular to the mitochondrial proteome (Kazak et al., 2013). Although our fractionation experiments did not allow us to observe any significant shift in size between the nuclear and mitochondrial OGG1, we cannot exclude that this second AUG could be used in particular conditions to favor nuclear import. OGG1 shares two characteristics with the proteins using several AUGs in frame: 1/ the first AUG has a suboptimal context for translation initiation, thus facilitating ribosomal sliding (leaky mRNA scanning) that could originate different polypeptides from the same transcript; and 2/ the 5'UTR is particularly long (350 nt compared to a normal length of around 200 nt) (Bazykin et al., 2011).

Interestingly, the three proteins involved in the GO system (David et al., 2007), dedicated to counteract the impact of the incorporation of 8-oxoG in DNA, OGG1, MTH1 and MUTYH share some characteristics. As for OGG1, several transcripts originated by alternative splicing have been identified for human MTH1 and MUTYH, (Oda et al., 1999; Ohtsubo et al., 2000) and some of them have two or three putative initiation codons, which are functional at least *in vitro*. Also as for *OGG1*, initiation of translation at the first AUG in their mRNAs gives rise to a protein containing a MTS, while initiation at the second AUG results in the loss of the MTS and yields a protein localized exclusively in the nucleus. Considering that all those proteins that are essential for the protection of mtDNA against the deleterious effects of 8-oxoG have evolved from very different families of proteins and do not have any sequence homology, it is striking to observe the very similar organization of the N-terminal sequences with the presence of several AUGs in frame. Although the molecular details have not been elucidated, alternative translation initiation has already been proposed to be the mechanism of choice for the generation of nuclear and mitochondrial isoforms of LIG3 (Lakshmipathy and Campbell, 1999). It is tempting to speculate that evolution has converged to this strategy in order to modulate the subcellular distribution of those enzymes. Further studies are required to better understand how the subcellular localization of the DNA glycosylase α-OGG1 and other BER proteins is modulated.

Our microscopy and biochemical observations show for the first time the association of α-OGG1 with the mtDNA in nucleoids. The use of 3-color structured illumination microscopy (3D-SIM) provided here a detailed view of this association and demonstrated the close proximity between the BER glycosylase and TFAM inside the mitochondrial network. While several proteins involved in DNA metabolism, such as Polγ, mtSSB and Twinkle have been found to associate with mtDNA only during replication in a highly regulated way (Rajala et al., 2014; Lewis et al., 2016), our experiments showed that the association of the glycosylase with the nucleoid is not linked to the replication state of the mtDNA but rather constitutive. Considering the highly compacted structure of mtDNA in nucleoids and the fact that the binding of TFAM to 8-oxoG containing DNA inhibits OGG1 activity *in vitro* (Canugovi et al., 2010), other proteins may be required to facilitate access of the DNA repair proteins to the mtDNA. A role for CSB in remodeling nucleoids by removing TFAM from DNA and facilitating the access of DNA repair machineries has been proposed (Boesch et al., 2012). This could explain the increase in 8-oxoG levels in mtDNA detected in *Csb -/-* mice

(Stevnsner et al., 2002; Osenbroch et al., 2009). α-OGG1 is strongly associated with a mitochondrial insoluble fraction, probably the inner mitochondrial membrane, as it resists extraction with up to 500 mM of NaCl and is protected from protease digestion coupled to an osmotic shock. This is in agreement with previous studies revealing the association of BER proteins and/or activities (DNA glycosylases, polymerase and ligase and to a minor extent the endonuclease) with an insoluble mitochondrial fraction (Stuart et al., 2005; Boesch et al., 2010). The mitochondrial nucleoids being themselves anchored to the inner mitochondrial membrane (Brown et al., 2011; Jakobs and Wurm, 2014; Gilkerson et al., 2013), this distribution of BER proteins could facilitate the efficiency of the DNA repair process.

Role of α-OGG1 in the maintenance of mitochondrial function

In our study, and in agreement with previous observations, a human cell line deficient in all OGG1 isoforms displays in response to a menadione treatment a higher loss of mitochondrial membrane potential and an accumulation of mitochondrial ROS, both indicators of mitochondrial dysfunction. The fact that the re-expression of the α-OGG1 isoform in those cells fully complemented those phenotypes (Fig. 6) suggests that this isoform is perfectly functional. The failure of the α-OGG1-ΔMTS protein, showing an exclusively nuclear localization, to complement the mitochondrial dysfunction of OGG1 deficient cells indicates that the presence of the protein inside mitochondria is required to maintain mitochondrial functions.

Under stress conditions, an increase in the fission versus fusion results in a fragmentation of the mitochondrial network, thus isolating the dysfunctional mitochondria that will be selectively removed by mitophagy. Furthermore, a perfect balance between fusion and fission is essential for the maintenance of mitochondrial health. A defect in either mitochondrial fusion or fission processes results in mtDNA instability (Busch et al., 2014, Garcia et al., 2017). The overexpression of α-OGG1 in human cells helps in preserving the mitochondrial network under oxidative stress conditions, as has also been observed in previous studies concerning the mouse Ogg1 (Torres-Gonzalez et al., 2014) and are in agreement with the general idea suggesting that DNA glycosylase activity is the rate-limiting step in the BER pathway (Hollenbach et al., 1999). The inability of the mutant protein α-OGG1(deltaMTS) in protecting mitochondrial network clearly indicates that the presence of the protein inside mitochondria is essential and it is not an indirect consequence of a better repair of nuclear DNA. Considering the major effect of the overexpression of α-OGG1 in protecting mitochondrial morphology, we cannot rule out that α-OGG1 has another role, independent on DNA repair, in mitochondrial fusion or fission. Indeed, the levels of mitochondrial proteins involved in fission, DRP and FIS1, have been reported to be reduced in cells overexpressing the mouse Ogg1 (Torres-Gonzalez et al., 2014), suggesting that the decrease in fission could account for the reduction in mitochondrial fragmentation observed. However, as fragmentation occurs as a consequence of mitochondrial dysfunction and is dependent on the loss of membrane potential, we can also imagine that this simply reflects the better health of mitochondria in cells overexpressing OGG1. In order to explore

whether the enzymatic activity of α-OGG1 is required for the maintenance of mitochondrial physiology after oxidative stress, we used a mutant in which Lys 249, essential for the cleavage of the N-glycosylic bond and the release 8-oxoG, is replaced by a Gln (K249Q) (Van der Kemp et al., 2004). This amino acid substitution does not induce any change in the structure of the protein (Bruner et al., 2000) nor in its subcellular localization (Fig. 2S). While overexpression of the wt α-OGG1 protects the mitochondrial network from fragmentation after exposure to menadione, the active site mutant K249Q failed to do so. This is in agreement with the results obtained with the OGG1 mutant R229Q. This mutation was initially identified in a leukemic cell line and results in a loss of enzymatic activity due to protein destabilization (Hyun et al., 2000; Hill and Evans, 2007). Targeting of the mutant protein MTS-hOGG1-R229Q to the mitochondria results in decreased mtDNA integrity and cellular survival after exposure to oxidative agents when compared to the wild type MTS-hOGG1 (Chatterjee et al, 2006). The fact that catalytically inactive α-OGG1 mutants could not preserve the mitochondrial morphology in cells exposed to oxidative stress make us favor the hypothesis that the observed mitochondrial dysfunctions are the consequence of the accumulation of 8-oxoG in the mitochondrial genome.

The presence of 8-oxoG has been proposed to be an important cause of mtDNA mutations and deletions, which accumulate with aging and during disease progression (Druzhyna et al., 2008). It is well accepted that the accumulation of 8-oxoG in DNA results in an increase in mutagenesis due to the misincorporation during DNA replication of adenine opposite 8-oxoG. An increase in mtDNA point mutations has been shown in yeast strains deficient for OGG1 (Singh et al., 2001). However, Halsne et al., reported that in *Ogg1*$^{-/-}$ mutant or in *Ogg1*$^{-/-}$ *Myh*$^{-/-}$ double mutant mice mtDNA mutation rates were not different from that of WT animals (Halsne et al. 2012). The experiments presented here show that menadione treatment rapidly induces mitochondrial dysfunction in OGG1-deficient cells, with around 40% of the cells showing a massive loss of membrane potential in less than 30 minutes. Those rapid effects could hardly be explained by an increase in mutagenesis, specially taking into account the high number of copies of mtDNA and the high degree of heteroplasmy and complementation between different mtDNA molecules. So, how can the failure to remove 8-oxoG affect mitochondrial functions? It has been proposed that Polymerase γ is blocked or paused by 8-oxoG (Graziewicz et al., 2007; Stojkovič et al., 2016), leading to the loss of mtDNA instead of mutagenesis. Although other replisome-associated proteins such as Twinkle or Primpol have been suggested to help the polymerase bypassing 8-oxoG (Garcia-Gomez et al., 2013; Bianchi et al., 2013; Stojkovič et al., 2016), other studies are required to conclude on the role of those proteins in processing damaged mtDNA. Several reports have shown that oxidative stress induces the degradation of the mtDNA and mtRNA (Crawford et al., 1997 and 1998; Abramova et al., 2000; Shokolenko et al., 2009; Rothfuss et al. 2010; Furda et al. 2012). It is interesting to note that while low levels of 8-oxoG have been detected in the circular molecule, fragmented mtDNA had a very high 8-oxodG content, which was further increased after oxidative stress (Suter and Richter, 1999). Thus, whether the accumulation of 8-oxoG in mitochondrial DNA in the absence of the DNA glycosylase activity of α-OGG1 represents a direct block for transcription or replication or it induces degradation of the DNA molecules remains to be further explored.

Materials and Methods

Cell lines, Plasmids construction, transfections, RNA interference and treatments

U2OS, HeLa and HEK cells were cultured at 37°C in Dulbecco's modified Eagle's medium (DMEM, Sigma ref D5671), supplemented with 10% fetal bovine serum (FBS) (Sigma ref F7524) and 5% penicillin/streptomycin (Gibco ref 15140122) in 5% CO_2.

pmTurquoise2-Mito was a gift from Dorus Gadella (Addgene plasmid # 36208)(Goedhart et al., 2012). α-OGG1 fusions to the FLAG epitope were generated by PCR, including the sequence coding for the FLAG in the reverse oligonucleotide, and cloned in the plasmid pCDNA3.1(-). The open reading frame of α-OGG1 was amplified by PCR to generate the fusion proteins OGG1(WT)-FLAG, OGG1(ΔMTS)-FLAG and OGG1(ΔNLS)-FLAG. The point mutations K249Q and G12E were introduced by site-directed mutagenesis from the hOGG1(WT)-FLAG construct, using the QuikChange Site-Directed Mutagenesis Kit (STRATAGENE). To facilitate the generation of stable cell lines, the same ORFs where cloned in the polycistronic pIRES2-AcGFP1 plasmid (CLONTECH) expressing the GFP in the second position of the cistron and thus allowing selecting the transfected cells expressing similar levels of the GFP by cell sorting. The oligonucleotides used to generate the different constructs are listed in Table S1

Cells were grown on coverslips, or on Ibidi µ-Slide 4 or 8 well plates for microscopy experiments and on T150 flasks for biochemical analysis. Transient and stable transfections were performed 24-48 hours after the seeding, using Lipofectamine 2000 (Invitrogen) and following a standard protocol with a ratio DNA/lipofectamine of 1µg/4µL. For stable cell lines expressing OGG1(WT)-FLAG or OGG1(ΔMTS)-FLAG from pIRES plasmids, the culture medium was supplemented with 400 µg/ml of G418.

For the siRNA-mediated depletion of hOGG1, U2OS cells were transfected with siRNA against hOGG1 (GGAUCAAGUAUGGACACUG) or AllStars Negative Control siRNA (QIAGEN) using Lipofectamine RNAiMAX (Invitrogen).

For the induction of an oxidative stress we used menadione at 50µM for 1 hour in DMEM without FBS and antibiotics. All dilutions were done in pre-warmed DMEM immediately before use.

Immunofluorescence and Confocal microscopy

For microscopy cells were plated in 4 or 8 Well µ-Slide from ibidi. For the staining of the mitochondrial network, cells were rinsed twice with DMEM and incubated with 200nM of MitoTracker RED CMXRos and/or MitoTracker Deep RED (purchased from ThermoFisher Scientific) diluted in complete DMEM for 30 min at 37°C. When indicated, DNA was stained with picogreen at 1/500 (Quant-iT™ PicoGreen™ dsDNA Reagent, ThermoFisher Scientific). Cells were fixed with 2% of formaldehyde for 20min at 37°C, rinsed with PBS and permeabilized at room temperature in PBS–0.1% Triton for 5min. Cells were incubated in blocking solution (PBS containing 0.1% Triton, 3% BSA and 1% normal goat serum) at 37 °C

for 1 hour or O.N. at 4°C. Cells were incubated for 1-2h at 37 °C with primary antibody diluted in blocking solution, washed three times for 5 min in PBS-0.1% Triton and further incubated with secondary Alexa Fluor fluorescent-conjugated antibodies (Molecular probes) diluted in blocking solution for 45min at 37°C. When indicated, nuclear DNA was counterstained with 1 µg/ml 4′,6′-diamidino-2-phenylindole (DAPI). The primary antibodies and the dilutions used were as follows: FLAG (SIGMA, F3165) 1:2000, TFAM (abcam, ab155240), 1:2000, CENPF (abcam, Ab5) 1:500, LC3B (Cell Signaling Technology, 27755) 1:250. EdU, 5-éthynyl-2'-déoxyuridine, was added to the medium at a concentration of 1 mM to label replicating cells and stained following the manufacturer's instructions (ThermoFischer Click-iT® EdU Alexa Fluor® 647).

Image acquisition was performed with a Leica confocal microscope SP8 with a 60x oil immersion objective or with a Nikon confocal A1 with a 63x oil immersion objective (NA 1,3 for both). Image analysis was performed with ImageJ (Schneider et al., 2012). Pearson correlation coefficients were calculated from 8 cells (around 1000 nucleoids) using the plugin JACOP (Bolte and Cordelières, 2006). Mitochondrial morphology alterations were characterized by applying the Kernel's algorithm (Koopman et al., 2005) to binarized images. This approach allows to measure morphology parameters for individual mitochondria such as the aspect ratio (AR), a measure of mitochondrial length, and the form factor (F), which is a combined measure of mitochondrial length and degree of branching.

Super-resolution microscopy

Structured illumination (3D-SIM) was performed using a rotary-stage OMX v3 system (Applied Precision—GE Healthcare), equipped with 3 EMCCD, Evolve cameras (Photometrics). Signals from all channels were realigned using fluorescent beads before each session of image acquisition. All images were acquired with a PlanApo 100×/1.4 oil objective at 125 nm intervals along the z axis. Resolution checked on 100 nm beads show 125nm, 125, 260 nm in x,y and z axis respectively. Channels alignment was realized with ImageJ using UnwarpJ plugin (Sánchez Sorzano, et al., 2005).

WCE, nuclear and mitochondrial extractions

Whole cell extracts were obtained from 10^6 U2OS cells. Cell pellets were resuspended in TpL buffer (TP lysis buffer: 20mM Tris HCl pH 7.5, 250mM NaCl, 1mM EDTA, protease inhibitors) and sonicated in a Bioruptor® bath (30″ on/30″ off pulses for 10 min at maximum intensity). After sonication the samples were centrifuged at 20000xg for 30 minutes at 4°C, the pellets discarded and the supernatants kept on ice.

Nuclear protein extracts were obtained from 10^6 U2OS with the Nuclei Isolation Kit: Nuclei EZ Prep (SIGMA), according to manufacturer's instructions.

Crude mitochondria extracts were prepared from $120x10^6$ U2OS cells, as described by Wieckowski et al. 2009 with few modifications. Briefly, cells at 90-95% of confluence were detached by trypsination and collected by centrifugation at 600×g for 7 minutes at 4°C. After one wash with ice-cold PBS the cells were

resuspended in ice-cold IB1 buffer (Isolation buffer 1: 225 mM mannitol, 75mM sucrose, 0.1 mM EGTA, 30mM Tris HCl pH 7.5) and disrupted with 15-30 strokes with a glass dounce homogenizer on ice. The integrity of the cells was checked under the microscope. The homogenate was centrifuged at 600xg for 7 minutes at 4°C. The supernatant was transferred into a pre-cooled ultracentrifuge vial and centrifuged at 7000xg for 12 minutes at 4°C. The supernatant was discarded and the pellet containing the mitochondria was gently resuspended in ice-cold IB2 buffer (Isolation buffer 2: 225 mM mannitol, 75mM sucrose, 30mM Tris HCl pH 7.5) and centrifuged again at 7000xg for 12 minutes at 4°C. The mitochondrial pellet was resuspended in IB2 buffer and re-pelleted at 10000xg for 12 minutes at 4°C. The crude mitochondrial pellet was resuspended in 120 µL of ice-cold MRB buffer (Mitochondrial Resuspension Buffer: 250mM mannitol, 0.5mM EGTA, and 5mM HEPES pH 7.4).

Protein contents of the different extracts were quantified by Bradford Assay.

Iodixanol gradient

Mitochondria isolated from HEK cells by differential and sucrose gradient centrifugation were treated with trypsin prior to lysis and fractionation on an iodixanol gradient as previously reported (Reyes et al., 2011). Briefly, cells were incubated in hypotonic buffer (20 mM HEPES pH 7.8/5 mM KCl/ 1.5 mM $MgCl_2$) on ice for 10 min and then homogenized with a tight-fitting homogenizer. Isotonic level was restored by the addition of 2.5X MSH (210 mM mannitol/70 mM sucrose/ 20 mM HEPES pH 7.8/ 2 mM EDTA pH 8.0). Nuclei and cell debris were spun down at low speed followed by high speed centrifugation to pellet crude mitochondria. Further purification of mitochondria was performed by loading crude mitochondria onto a discontinuous 1.5/1.0 M sucrose gradient and collecting purified mitochondria from its interphase. The organelles were then lysed with 0.4% DDM in 1X MSH and loaded onto a 20-45% self-forming continuous iodixanol gradient. After centrifugation at 100 000 g for 14 h, 18 fractions of 450 µl were collected and protein and DNA were extracted from them and analyzed by Southern and Western blotting, respectively. A mitochondrial DNA fragment amplified by PCR with specific oligos (Table S1) was incubated with DNA-labeling beads (GE Healthcare) in the presence of 50mCi of [a-32P] dCTP (3000 Ci/mmol, Perkin Elmer) for 30 min. Then, the Southern blot was hybridized to this mtDNA specific probe by overnight incubation at 65°C in 7% SDS/ 0.25M sodium phosphate buffer (pH 7.4). Post hybridization washes were 1XSSC followed by 1XSSC/ 0.1% SDS twice for 30 min at 65°C. Filters were exposed to phosphorscreens and scanned using a Typhoon phosporimager (GE Healthcare). The Western blots were incubated with antibodies against TFAM, the soluble glycyl-tRNA synthetase GARS and α-OGG1.

Proteinase K and trypsin partial digestion

25µg of mitochondrial extracts were incubated for 5 min at 4°C in 1 mL of MBR buffer with 1 mg/ml of BSA, with a final concentration of 5 or 25 µg/mL of Proteinase K (PK). When indicated a pretreatment with 1% of Triton- X100 for 5 min at 4°C was performed before the incubation with PK. PK was inactivated on ice by

adding 10 mM PMSF for 5 min. The samples were then centrifuged at 14000rpm for 10' at 4°C and the supernatant discarded. The resulting pellets were resuspended in 50 µL of MBR. Untreated mitochondrial extracts were used as a control.

Trypsin digestion

Mitochondria from HEK cells (2mg/ml) purified with sucrose gradients as described above were resuspended in either isotonic (20 mM HEPES pH 7.8, 2 mM EDTA, 210 mM mannitol, 70 mM sucrose) or hypotonic (10 mM HEPES pH 7.8) buffer in order to disrupt the mitochondrial outer membrane and then or left untreated or treated with 100 µg/ml of trypsin at room temperature for 30 min in order to digest proteins that localize in the outer membrane or the intermembrane space while protecting those in the mitochondrial matrix and the mitochondrial inner membrane facing the matrix side. Purified mitochondria were alternatively treated with 200 or 500 mg/ml digitonin in isotonic buffer for 10 min at 4°C prior to trypsin treatment, as previously reported (Reyes et al., 2011) as an alternative method of mitochondrial outer membrane disruption and digestion of proteins from the outer membrane or the intermembrane space. After washing and pelleting mitochondria three times, the organelles were lysed with 1% SDS in isotonic buffer. TOM20, TIM23, SDHA and EFTB were used as markers for the mitochondrial outer membrane, intermembrane space, mitochondrial inner membrane and mitochondrial matrix, respectively.

Extraction of mitochondrial membranes

Sucrose-gradient purified mitochondria from HEK cells (2 mg/ml) obtained as above were sonicated for 1 min on ice followed by centrifugation at 10.000 g for 10 min at 4°C. The supernatant was treated with 150 or 500 mM NaCl or 2% SDS on ice for 30 min followed by centrifugation at 122,000 g for 30 min at 4°C. Supernatants containing the soluble fractions were recovered and pellets with membrane-associated proteins were suspended in equal volume of isotonic buffer containing 0,2% SDS, as previously described (Martinez Lyons et al., 2016). TOM20 and CS were used as controls of integral membrane and soluble protein, respectively.

Western blotting analysis

Aliquots from each cell extracts were denatured by heating at 95 °C for 5 min. Loading of the extracts was normalized by protein content and 10-20 µg of protein extracts were separated in 10% SDS-acrylamide gel and transferred onto a nitrocellulose membrane. To confirm the amounts of protein in each lane, membranes were stained with Ponceau red and then blocked in 8% milk in PBS with 0.1% Tween 20 (TPBS) for 30 min at RT or O.N. at 4°C. After the blocking step the membranes were incubated for 90 min at RT with primary antibodies in 3% milk-PBS. All the antibodies used are listed in Table S2. After three 5 min washings with PBS, blots were incubated 45 min at RT with fluorescently labeled secondary antibodies: anti-Rabbit-800 (ref 05060-250), anti-Mouse-800 (ref 05061-250), anti-Rabbit-700 (ref 05054-250) and/or anti-Mouse-700 (ref 050055-250) (Diagomics) diluted 1:10000 in 2% milk-TPBS or HRP conjugated secondary antibodies

(Promega anti-Rabbit W401B, anti-Mouse W402B) 1:5000 and then washed 3 times with TPBS for 7-10' min. The analysis of the images was performed by scanning the membrane at 800 and 700nm simultaneously with an Odyssey® CLx or by exposure to X-ray films.

Determination of mitochondrial mass, membrane potential and ROS production

Analysis of mitochondrial mass, mitochondrial membrane potential (MMP) and intramitochondrial ROS (mtROS) production were performed by flow cytometry (BD LSRII) or microplate reader (CLARIOstar - BMG Labtech).

For Flow cytometry analysis 0.4exp6 U2OS were seeded in a 6 well plate and transfected with siOGG1 or with siAllStar as previously described. 72h after transfection the cells were treated 1h at 37°C with 50µM of menadione. To evaluate mtROS, U2OS cells were incubated with 5µM of MitoSOX® Red Mitochondrial Superoxide Indicator (ThermoFisher, ref. M36008) in PBS-BSA 0.4% for 10 min at 37°C protected from light, harvested with trypsin and directly analyzed. For MMP analysis cells were incubated with 100nM of MitoTracker GREEN FM (ThermoFisher, ref. M7514) for 30 min at 37°C, rinsed once and stained with 100 nM of TMRE (Tetramethylrhodamine, Ethyl Ester, Perchlorate, ThermoFischer, ref. T669) diluted in PBS-BSA 0.4% for 15', 37°C protected from light. The cells were then harvested with trypsin and directly analyzed. For each sample, at least 50.000 cells were analyzed. Experiments were performed three times with similar results.

For plate reader measurements 10000 cells were reverse transfected with siOGG1 or siAllStars in a 96-well microplate for fluorescence assays, black-walled and with clear-bottom (Greiner Bio-One, ref. 655090). The cells were treated with 25 or 50 µM of menadione for 1h at 37°C and then rinsed once with complete DMEM. For the analysis of mtROS production after the chemical treatment the cells were stained for 10 min maximum with MitoSOX® Red, 5µM and Hoecst 33342 1:1000 diluted in pre-warmed PBS ($+Ca^{2+}$ and Mg^{2+}), the PBS was then replaced with 199 µl medium before the acquisition. To evaluate the MMP the cells were stained before the chemical treatment with 100 nM of TMRE and 100 nM of MitoTracker GREEN for 30 min at 37°C protected from light.

OGG1 glycosylase activity

A single-stranded 34-mer DNA containing an 8-oxoG at position 16 was 5 -end labelled with Cy5 and hybridized to the complementary oligonucleotide containing a cytosine opposite the lesion, yielding the 8-oxoG:C duplexes. Reactions were carried out at 37°C in a total volume of 14 µl, containing the specified amount of protein extract and 150 fmol of DNA probe. The reaction buffer was 22 mM Tris–HCl pH 7.4, 110 mM NaCl, 2.5 mM EDTA, 1 mg/ml BSA and 5% glycerol. Reaction mixtures containing 8-oxoG:C probe were incubated at 37 ◦C for 1 h, then NaOH (0.1 N final concentration) was added and the mixture was further incubated for 15 min at 37 ◦C and stopped by adding 6 µl of formamide dye (80% formamide, 10 mM EDTA, 0.02% bromophenol blue), followed by heating for 5 min at 95 ◦C. The products of the reactions were

resolved by denaturing 7 M urea – 20% polyacrylamide gel electrophoresis. Gels were scanned using a Typhoon Multi-format Imager (GE Healthcare Life Sciences).

Acknowledgments

We thank the scientific and technical assistance of the Microscopy, Flow cytometry and Molecular Biology facilities of the IRCM Institute. We thank Samantha Lewis (Nunnari lab) for her help in the optimization of the protocol for visualization of replicating nucleoids. We would like to thank Paul-Henri Romeo, Christophe Carles and Chantal Desmaze for critically reading the manuscript. This research was supported by grants from Ligue contre le cancer, Electricité de France and the CEA (Impulsion).

Author contributions

D. Lia performed experiments and analysed the data. A. Reyes performed experiments for Fig 1 (B and C) and 2 (E) and edited the manuscript. JT de Melo performed preliminary experiments. T. Piolot performed SIM experiments presented in Fig 2 (C and D). J. Baijer analysed flow cytometry data (Fig. 5). J.P. Radicella edited the manuscript. A. Campalans conceived the study, designed and performed experiments, analysed the data and wrote the paper.

References

Abramova, N. E., Davies, K. J. A. and Crawford, D. R. (2000). Polynucleotide degradation during early stage response to oxidative stress is specific to mitochondria. *Free Radic. Biol. Med.* **28**, 281–288.

Alam, T. I., Kanki, T., Muta, T., Ukaji, K., Abe, Y., Nakayama, H., Takio, K., Hamasaki, N. and Kang, D. (2003). Human mitochondrial DNA is packaged with TFAM. *Nucleic Acids Res.* **31**, 1640–1645.

Audebert, M., Charbonnier, J. B., Boiteux, S. and Radicella, J. P. (2002). Mitochondrial targeting of human 8-oxoguanine DNA glycosylase hOGG1 is impaired by a somatic mutation found in kidney cancer. *DNA Repair (Amst).* **1**, 497–505.

Bazykin, G. A. and Kochetov, A. V. (2011). Alternative translation start sites are conserved in eukaryotic genomes. *Nucleic Acids Res.* **39**, 567–577.

Berquist, B. R., Canugovi, C., Sykora, P., Wilson, D. M. and Bohr, V. A. (2012). Human Cockayne syndrome B protein reciprocally communicates with mitochondrial proteins and promotes transcriptional elongation. *Nucleic Acids Res.* **40**, 8392–8405.

Boesch, P., Ibrahim, N., Dietrich, A. and Lightowlers, R. N. (2010). Membrane association of mitochondrial DNA facilitates base excision repair in mammalian mitochondria. *Nucleic Acids Res* **38**, 1478–1488.

Bolte, S. and Cordelieres, F. P. (2006). A guided tour into subcellular colocalisation analysis in light microscopy. *J. Microsc.* **224**, 13–232.

Brown, T. A., Tkachuk, A. N., Shtengel, G., Kopek, B. G., Bogenhagen, D. F., Hess, H. F. and Clayton, D. A. (2011). Superresolution Fluorescence Imaging of Mitochondrial Nucleoids Reveals Their Spatial Range, Limits, and Membrane Interaction. *Mol. Cell. Biol.* **31**, 4994–5010.

Bruner, S. D., Norman, D. P. and Verdine, G. L. (2000). Structural basis for recognition and repair of the endogenous mutagen 8-oxoguanine in DNA. *Nature* **403**, 859–66.

Busch, K. B., Kowald, A. and Spelbrink, J. N. (2014). Quality matters: how does mitochondrial network dynamics and quality control impact on mtDNA integrity? *Philos. Trans. R. Soc. Lond. B. Biol. Sci.* **369**, 20130442.

Canugovi, C., Maynard, S., Bayne, A.-C. V., Sykora, P., Tian, J., de Souza-Pinto, N. C., Croteau, D. L. and Bohr, V. A. (2010). The mitochondrial transcription factor A functions in mitochondrial base excision repair. *DNA Repair (Amst).* **9**, 1080–1089.

Chatterjee, A., Mambo, E., Zhang, Y., Deweese, T. and Sidransky, D. (2006). Targeting of mutant hogg1 in mammalian mitochondria and nucleus: effect on cellular survival upon oxidative stress. *BMC Cancer* **6**, 235.

Crawford, D. R., Wang, Y., Schools, G. P., Kochheiser, J. and Davies, K. J. A. (1997). Down-regulation of mammalian mitochondrial RNAs during oxidative stress. *Free Radic. Biol. Med.* **22**, 551–559.

Crawford, D. R., Abramova, N. E. and Davies, K. J. A. (1998). Oxidative stress causes a general, calcium-dependent degradation of mitochondrial polynucleotides. *Free Radic. Biol. Med.* **25**, 1106–1111.

David, S. S., O'Shea, V. L. and Kundu, S. (2007). Base-excision repair of oxidative DNA damage. *Nature* **447**, 941–950.

de Souza-Pinto, N. C., Hogue, B. A. and Bohr, V. A. (2001). DNA repair and aging in mouse liver: 8-oxodG glycosylase activity increase in mitochondrial but not in nuclear extracts. *Free Radic Biol Med* **30**, 916–923.

Dobson, A. W., Xu, Y., Kelley, M. R., LeDoux, S. P. and Wilson, G. L. (2000a). Enhanced mitochondrial DNA repair and cellular survival after oxidative stress by targeting the human 8-oxoguanine glycosylase repair enzyme to mitochondria. *J Biol Chem* **275**, 37518–37523.

Dobson, A. W., Xu, Y., Kelley, M. R., LeDoux, S. P. and Wilson, G. L. (2000b). Enhanced mitochondrial DNA repair and cellular survival after oxidative stress by targeting the human 8-oxoguanine glycosylase repair enzyme to mitochondria. *J. Biol. Chem.* **275**, 37518–37523.

Dobson, A. W., Grishko, V., LeDoux, S. P., Kelley, M. R., Wilson, G. L. and Gillespie, M. N. (2002). Enhanced mtDNA repair capacity protects pulmonary artery endothelial cells from oxidant-mediated death. *Am. J. Physiol. Lung Cell. Mol. Physiol.* **283**, L205–10.

Druzhyna, N. M., Musiyenko, S. I., Wilson, G. L. and LeDoux, S. P. (2005). Cytokines induce nitric oxide-mediated mtDNA damage and apoptosis in oligodendrocytes: Protective role of targeting 8-oxoguanine glycosylase to mitochondria. *J. Biol. Chem.* **280**, 21673–21679.

Druzhyna, N. M., Wilson, G. L. and Ledoux, S. P. (2009). Mitochondrial DNA repair in aging and disease. *Mech Ageing Dev* **129**, 383–390.

Furda, A. M., Marrangoni, A. M., Lokshin, A. and Van Houten, B. (2012). Oxidants and not alkylating agents induce rapid mtDNA loss and mitochondrial dysfunction. *DNA Repair (Amst).* **11**, 684–692.

673 **Furihata, C.** (2015). An active alternative splicing isoform of human mitochondrial 8-oxoguanine DNA
674 glycosylase (OGG1). *Genes Environ.* **37**, 21.

675 **Garc??a-G??mez, S., Reyes, A., Mart??nez-Jim??nez, M. I., Chocr??n, E. S., Mour??n, S.,**
676 **Terrados, G., Powell, C., Salido, E., M??ndez, J., Holt, I. J., et al.** (2013). PrimPol, an Archaic
677 Primase/Polymerase Operating in Human Cells. *Mol. Cell* **52**, 541–553.

678 **Garcia, I., Jones, E., Ramos, M., Innis-Whitehouse, W. and Gilkerson, R.** (2017). The little big
679 genome: the organization of mitochondrial DNA. *Front. Biosci. (Landmark Ed.* **22**, 710–721.

680 **Garcia-Gomez, S., Reyes, A., Martinez-Jimenez, M. I., Chocron, E. S., Mouron, S., Terrados, G.,**
681 **Powell, C., Salido, E., Mendez, J., Holt, I. J., et al.** (2013). PrimPol, an Archaic
682 Primase/Polymerase Operating in Human Cells. *Mol. Cell* **52**, 541–553.

683 **Gilkerson, R. W., Schon, E. A., Hernandez, E. and Davidson, M. M.** (2008). Mitochondrial nucleoids
684 maintain genetic autonomy but allow for functional complementation. *J. Cell Biol.* **181**, 1117–1128.

685 **Gilkerson, R., Bravo, L., Garcia, I., Gaytan, N. and Herrera, A.** (2013). The Mitochondrial Nucleoid :
686 Integrating. *Cold Spring Harb Perspect Biol* **5**, 1–10.

687 **Goedhart, J., von Stetten, D., Noirclerc-Savoye, M., Lelimousin, M., Joosen, L., Hink, M. A., van**
688 **Weeren, L., Gadella, T. W. J. and Royant, A.** (2012). Structure-guided evolution of cyan
689 fluorescent proteins towards a quantum yield of 93%. *Nat. Commun.* **3**, 751.

690 **Graziewicz, M. A., Bienstock, R. J. and Copeland, W. C.** (2007). The DNA polymerase γ Y955C
691 disease variant associated with PEO and parkinsonism mediates the incorporation and translesion
692 synthesis opposite 7,8-dihydro-8-oxo-2′-deoxyguanosine. *Hum. Mol. Genet.* **16**, 2729–2739.

693 **Griffiths, L. M., Swartzlander, D., Meadows, K. L., Wilkinson, K. D., Corbett, A. H. and Doetsch, P.**
694 **W.** (2009). Dynamic compartmentalization of base excision repair proteins in response to nuclear
695 and mitochondrial oxidative stress. *Mol Cell Biol* **29**, 794–807.

696 **Halsne, R., Esbensen, Y., Wang, W., Scheffler, K., Suganthan, R., Bjørås, M. and Eide, L.** (2012).
697 Lack of the DNA glycosylases MYH and OGG1 in the cancer prone double mutant mouse does not
698 increase mitochondrial DNA mutagenesis. *DNA Repair (Amst).* **11**, 278–285.

699 **Harbauer, A. B., Opali ska, M., Gerbeth, C., Herman, J. S., Rao, S., Schonfisch, B., Guiard, B.,**
700 **Schmidt, O., Pfanner, N. and Meisinger, C.** (2014). Cell cycle-dependent regulation of
701 mitochondrial preprotein translocase. *Science (80-.).* **346**, 1109–1113.

702 **Hill, J. W. and Evans, M. K.** (2007). A novel R229Q OGG1 polymorphism results in a thermolabile
703 enzyme that sensitizes KG-1 leukemia cells to DNA damaging agents. *Cancer Detect. Prev.* **31**,
704 237–243.

705 **Hollenbach, S., Dhénaut, A., Eckert, I., Radicella, J. P. and Epe, B.** (1999). Overexpression of Ogg1 in
706 mammalian cells: Effects on induced and spontaneous oxidative DNA damage and mutagenesis.
707 *Carcinogenesis* **20**, 1863–1868.

708 **Hyun, J. W., Choi, J. Y., Zeng, H. H., Lee, Y. S., Kim, H. S., Yoon, S. H. and Chung, M. H.** (2000).
709 Leukemic cell line, KG-1 has a functional loss of hOGG1 enzyme due to a point mutation and 8-
710 hydroxydeoxyguanosine can kill KG-1. *Oncogene* **19**, 4476–9.

Jakobs, S. and Wurm, C. A. (2014). Super-resolution microscopy of mitochondria. *Curr. Opin. Chem. Biol.* **20**, 9–15.

Kazak, L., Reyes, A. and Holt, I. J. (2012). Minimizing the damage: repair pathways keep mitochondrial DNA intact. *Nat. Rev. Mol. Cell Biol.* **13**, 726–726.

Kazak, L., Reyes, A., Duncan, A. L., Rorbach, J., Wood, S. R., Brea-Calvo, G., Gammage, P. A., Robinson, A. J., Minczuk, M. and Holt, I. J. (2013). Alternative translation initiation augments the human mitochondrial proteome. *Nucleic Acids Res.* **41**, 2354–2369.

Kim, S. J., Cheresh, P., Williams, D., Cheng, Y., Ridge, K., Schumacker, P. T., Weitzman, S., Bohr, V. A. and Kamp, D. W. (2014). Mitochondria-targeted Ogg1 and aconitase-2 prevent oxidant-induced mitochondrial DNA damage in alveolar epithelial cells. *J. Biol. Chem.* **289**, 6165–6176.

Kukat, C., Wurm, C. a, Spåhr, H., Falkenberg, M., Larsson, N.-G. and Jakobs, S. (2011). Super-resolution microscopy reveals that mammalian mitochondrial nucleoids have a uniform size and frequently contain a single copy of mtDNA. *Proc. Natl. Acad. Sci. U. S. A.* **108**, 13534–13539.

Lakshmipathy, U. and Campbell, C. (1999). The human DNA ligase III gene encodes nuclear and mitochondrial proteins. *Mol Cell Biol* **19**, 3869–3876.

Legros, F., Malka, F., Frachon, P., Lombes, A. and Rojo, M. (2004). Organization and dynamics of human mitochondrial DNA. *J Cell Sci* **117**, 2653–2662.

Leon, J., Sakumi, K., Castillo, E., Sheng, Z., Oka, S. and Nakabeppu, Y. (2016). 8-Oxoguanine accumulation in mitochondrial DNA causes mitochondrial dysfunction and impairs neuritogenesis in cultured adult mouse cortical neurons under oxidative conditions. *Sci. Rep.* **6**, 22086.

Lewis, S. C., Uchiyama, L. F. and Nunnari, J. (2016). ER-mitochondria contacts couple mtDNA synthesis with mitochondrial division in human cells. *Science (80-.).* **353**, aaf5549.

Martinez Lyons, A., Ardissone, A., Reyes, A., Robinson, A. J., Moroni, I., Ghezzi, D., Fernandez-Vizarra, E. and Zeviani, M. (2016). COA7 (C1orf163/RESA1) mutations associated with mitochondrial leukoencephalopathy and cytochrome c oxidase deficiency. *J. Med. Genet.* **53**, 846–849.

Mishra, P. and Chan, D. C. (2014). Mitochondrial dynamics and inheritance during cell division, development and disease. **15**, 634–646.

Model, K., Meisinger, C. and Kühlbrandt, W. (2008). Cryo-Electron Microscopy Structure of a Yeast Mitochondrial Preprotein Translocase. *J. Mol. Biol.* **383**, 1049–1057.

Nishioka, K., Ohtsubo, T., Oda, H., Fujiwara, T., Kang, D., Sugimachi, K. and Nakabeppu, Y. (1999). Expression and differential intracellular localization of two major forms of human 8-oxoguanine DNA glycosylase encoded by alternatively spliced OGG1 mRNAs. *Mol Biol Cell* **10**, 1637–1652.

Oda, H., Taketomi, A., Maruyama, R., Itoh, R., Nishioka, K., Yakushiji, H., Suzuki, T., Sekiguchi, M. and Nakabeppu, Y. (1999). Multi-forms of human MTH1 polypeptides produced by alternative translation initiation and single nucleotide polymorphism. *Nucleic Acids Res* **27**, 4335–4343.

Ogawa, A., Watanabe, T., Shoji, S. and Furihata, C. (2015). Enzyme kinetics of an alternative splicing isoform of mitochondrial 8-oxoguanine DNA glycosylase, OGG1-1b, and compared with the nuclear OGG1-1a. *J. Biochem. Mol. Toxicol.* **29**, 49–56.

Ohtsubo, T. (2000). Identification of human MutY homolog (hMYH) as a repair enzyme for 2-hydroxyadenine in DNA and detection of multiple forms of hMYH located in nuclei and mitochondria. *Nucleic Acids Res.* **28**, 1355–1364.

Oka, S., Ohno, M., Tsuchimoto, D., Sakumi, K., Furuichi, M. and Nakabeppu, Y. (2008). Two distinct pathways of cell death triggered by oxidative damage to nuclear and mitochondrial DNAs. *Embo J* **27**, 421–432.

Oka, S., Leon, J., Tsuchimoto, D., Sakumi, K. and Nakabeppu, Y. (2014). MUTYH, an adenine DNA glycosylase, mediates p53 tumor suppression via PARP-dependent cell death. *Oncogenesis* **3**, e121.

Osenbroch, P. O., Auk-Emblem, P., Halsne, R., Strand, J., Forstrøm, R. J., Van Der Pluijm, I. and Eide, L. (2009). Accumulation of mitochondrial DNA damage and bioenergetic dysfunction in CSB defective cells. *FEBS J.* **276**, 2811–2821.

Rachek, L. I., Grishko, V. I., Musiyenko, S. I., Kelley, M. R., LeDoux, S. P. and Wilson, G. L. (2002). Conditional targeting of the DNA repair enzyme hOGG1 into mitochondria. *J Biol Chem* **277**, 44932–44937.

Rajala, N., Gerhold, J. M., Martinsson, P., Klymov, A. and Spelbrink, J. N. (2014). Replication factors transiently associate with mtDNA at the mitochondrial inner membrane to facilitate replication. *Nucleic Acids Res.* **42**, 952–967.

Reyes, A., He, J., Mao, C. C., Bailey, L. J., Di Re, M., Sembongi, H., Kazak, L., Dzionek, K., Holmes, J. B., Cluett, T. J., et al. (2011). Actin and myosin contribute to mammalian mitochondrial DNA maintenance. *Nucleic Acids Res.* **39**, 5098–5108.

Richter, C., Park, J. W. and Ames, B. N. (1988). Normal oxidative damage to mitochondrial and nuclear DNA is extensive. *Proc. Natl. Acad. Sci. U. S. A.* **85**, 6465–7.

Rothfuss, O., Gasser, T. and Patenge, N. (2009). Analysis of differential DNA damage in the mitochondrial genome employing a semi-long run real-time PCR approach. *Nucleic Acids Res.* **38**,.

Santos, J. H., Hunakova, L., Chen, Y., Bortner, C. and Van Houten, B. (2003). Cell sorting experiments link persistent mitochondrial DNA damage with loss of mitochondrial membrane potential and apoptotic cell death. *J. Biol. Chem.* **278**, 1728–1734.

Schneider, C. A., Rasband, W. S. and Eliceiri, K. W. (2012). NIH Image to ImageJ: 25 years of image analysis. *Nat. Methods* **9**, 671–675.

Schon, E. A. and Gilkerson, R. W. (2010). Functional complementation of mitochondrial DNAs: Mobilizing mitochondrial genetics against dysfunction. *Biochim. Biophys. Acta - Gen. Subj.* **1800**, 245–249.

Schulz, C., Schendzielorz, A. and Rehling, P. (2015). Unlocking the presequence import pathway. *Trends Cell Biol.* **25**, 265–275.

Shigenaga, M. K., Hagen, T. M. and Ames, B. N. (1994). Oxidative damage and mitochondrial decay in aging. *Proc. Natl. Acad. Sci. U. S. A.* **91**, 10771–8.

Shokolenko, I., Venediktova, N., Bochkareva, A., Wilson, G. L. and Alexeyev, M. F. (2009). Oxidative stress induces degradation of mitochondrial DNA. *Nucleic Acids Res.* **37**, 2539–48.

Simsek, D., Furda, A., Gao, Y., Artus, J., Brunet, E., Hadjantonakis, A. K., Van Houten, B., Shuman, S., McKinnon, P. J. and Jasin, M. (2011). Crucial role for DNA ligase III in mitochondria but not in Xrcc1-dependent repair. *Nature* **471**, 245–248.

Singh, K. K., Sigala, B., Sikder, H. A. and Schwimmer, C. (2001). Inactivation of Saccharomyces cerevisiae OGG1 DNA repair gene leads to an increased frequency of mitochondrial mutants. *Nucleic Acids Res.* **29**, 1381–8.

Sorzano, C. Ó. S., Thévenaz, P. and Unser, M. (2005). Elastic registration of biological images using vector-spline regularization. *IEEE Trans. Biomed. Eng.* **52**, 652–663.

Stevnsner, T., Thorslund, T., de Souza-Pinto, N. C. and Bohr, V. A. (2002a). Mitochondrial repair of 8-oxoguanine and changes with aging. *Exp Gerontol* **37**, 1189–1196.

Stevnsner, T., Nyaga, S., de Souza-Pinto, N. C., van der Horst, G. T. J., Gorgels, T. G. M. F., Hogue, B. a, Thorslund, T. and Bohr, V. a (2002b). Mitochondrial repair of 8-oxoguanine is deficient in Cockayne syndrome group B. *Oncogene* **21**, 8675–82.

Stojkovič, G., Makarova, A. V., Wanrooij, P. H., Forslund, J., Burgers, P. M. and Wanrooij, S. (2016). Oxidative DNA damage stalls the human mitochondrial replisome. *Sci. Rep.* **6**, 28942.

Stuart, J. A., Mayard, S., Hashiguchi, K., Souza-Pinto, N. C. and Bohr, V. A. (2005). Localization of mitochondrial DNA base excision repair to an inner membrane-associated particulate fraction. *Nucleic Acids Res* **33**, 3722–3732.

Suter, M. and Richter, C. (1999). Fragmented Mitochondrial DNA Is the Predominant Carrier of Oxidized DNA Bases †. *Biochemistry* **38**, 459–464.

Swartzlander, D. B., Griffiths, L. M., Lee, J., Degtyareva, N. P., Doetsch, P. W. and Corbett, A. H. (2010). Regulation of base excision repair: Ntg1 nuclear and mitochondrial dynamic localization in response to genotoxic stress. *Nucleic Acids Res* **38**, 3963–3974.

Swartzlander, D. B., McPherson, A. J., Powers, H. R., Limpose, K. L., Kuiper, E. G., Degtyareva, N. P., Corbett, A. H. and Doetsch, P. W. (2016). Identification of SUMO modification sites in the base excision repair protein, Ntg1. *DNA Repair (Amst).* **48**, 51–62.

Sykora, P., Kanno, S., Akbari, M., Kulikowicz, T., Baptiste, B. A., Leandro, G. S., Lu, H., Tian, J., May, A., Becker, K. A., et al. (2017a). DNA polymerase beta participates in mitochondrial DNA repair. *Mol. Cell. Biol.* MCB.00237–17.

Sykora, P., Kanno, S., Akbari, M., Kulikowicz, T., Baptiste, B. A., Leandro, G. S., Lu, H., Tian, J., May, A., Becker, K. A., et al. (2017b). DNA polymerase beta participates in mitochondrial DNA repair. *Mol. Cell. Biol.* **37**, MCB.00237–17.

Takao, M., Aburatani, H., Kobayashi, K. and Yasui, A. (1998). Mitochondrial targeting of human DNA glycosylases for repair of oxidative DNA damage. *Nucleic Acids Res* **26**, 2917–2922.

Torres-Gonzalez, M., Gawlowski, T., Kocalis, H., Scott, B. T. and Dillmann, W. H. (2014). Mitochondrial 8-oxoguanine glycosylase decreases mitochondrial fragmentation and improves mitochondrial function in H9C2 cells under oxidative stress conditions. *AJP Cell Physiol.* **306**, C221–C229.

Tress, M. L., Abascal, F. and Valencia, A. (2017). Alternative Splicing May Not Be the Key to Proteome Complexity. *Trends Biochem. Sci.* **42**, 98–110.

Trifunovic, Aleksandra, Wredenberg, Anna, Maria Falkenberg1, Johannes N. Spelbrink3, Anja T. Rovio3, Carl E. Bruder4, Mohammad Bohlooly-Y4, Sebastian Gidlo¨ f1, 2, Anders Oldfors5, Rolf Wibom6, Jan To¨ rnell4, Howard T. Jacobs3 & Nils-Go¨ran Larsson, 2 (2004). Premature ageing in mice expressing defective mitochondrial DNA polymerase. *Nature* **429**, 417–423.

Van Damme, P., Gawron, D., Van Criekinge, W. and Menschaert, G. (2014). N-terminal Proteomics and Ribosome Profiling Provide a Comprehensive View of the Alternative Translation Initiation Landscape in Mice and Men. *Mol. Cell. Proteomics* **13**, 1245–1261.

van der Kemp, P. A., Charbonnier, J. B., Audebert, M. and Boiteux, S. (2004). Catalytic and DNA-binding properties of the human Ogg1 DNA N-glycosylase/AP lyase: Biochemical exploration of H270, Q315 and F319, three amino acids of the 8-oxoguanine-binding pocket. *Nucleic Acids Res.* **32**, 570–578.

Wang, W., Esbensen, Y., Kunke, D., Suganthan, R., Rachek, L., Bjoras, M. and Eide, L. (2011). Mitochondrial DNA damage level determines neural stem cell differentiation fate. *J Neurosci* **31**, 9746–9751.

Wieckowski, M. R., Giorgi, C., Lebiedzinska, M., Duszynski, J. and Pinton, P. (2009). Isolation of mitochondria-associated membranes and mitochondria from animal tissues and cells. *Nat. Protoc.* **4**, 1582–1590.

Yakes, F. M. and Van Houten, B. (1997). Mitochondrial DNA damage is more extensive and persists longer than nuclear DNA damage in human cells following oxidative stress. *Proc Natl Acad Sci U S A* **94**, 514–519.

Yogev, O. and Pines, O. (2011). Dual targeting of mitochondrial proteins: Mechanism, regulation and function. *Biochim. Biophys. Acta - Biomembr.* **1808**, 1012–1020.

Zhang, L., Chan, S. S. L. and Wolff, D. J. (2011). Mitochondrial disorders of DNA Polymerase 7 dysfunction: From anatomic to molecular pathology diagnosis. *Arch. Pathol. Lab. Med.* **135**, 925–934.

Table S1. List of oligonucleotides used in this study

Primer name	Constrcut	Primer sequence
α-OGG1F-WT (Forward)	α-OGG1-WT α-OGG1-ΔNLS	5'-TCG AAT TCG GGCGGTGCTGCTGTGGAAATG CCT GCC CGC GCG CTT C -3'
α-OGG1F-ΔMTS (Forward)	α-OGG1-ΔMTS	5'- T5'- TCG AAT TCG GGCATGGGGCATCGTACTCTAG-3'
α-OGG1R-FLAG (reverse)	α-OGG1-WT α-OGG1-ΔMTS	5'- G5'- GC GGA TCC CTA CTT ATC GTC GTC ATC CTT GTA ATC GGC CCT GCC TTC CGG CCC TTT GGA AC-3'
α-OGG1R-ΔNLS-FLAG (reverse)	α-OGG1-ΔNLS	5'- GC GGA TCC CTA CTT ATC GTC GTC ATC CTT GTA ATC GGC CCT TGC TGG TGG CTC CTG AGC ATG-3'
α-OGG1F-G12E (Forward)	For Site Directed Mutagenesis	5'- CTT CTG CCC AGG CGC ATG GAG CAT CGT ACT CTA GCC TC-3'
α-OGG1R-G12E (Reverse)	For Site Directed Mutagenesis	5'- GAG GCT AGA GTA CGA TGC TCC ATG CGC CTG GGC AGA AG-3'
α-OGG1F-K249Q (Forward)	For Site Directed Mutagenesis	5'-GGA GTG GGC ACC CAG GTG GCT GAC TGC-3'
α-OGG1R-K249Q (Reverse)	For Site Directed Mutagenesis	5'-GCA GTC AGC CAC CTG GGT GCC CAC TCC -3'
HsOGG1a-Mut (Forward)	silent mutations siRNA	5' – CCAGGTGTGGACGTTGACTCAGACTGAGGAGCAG – 3'
HsOGG1a-Mut (Reverse)	silent mutations siRNA	5' – ACGTCCACACCTGGTCAGCTAGTACACCACTCCAGTGTG – 3'
mtDNA probe F	For southern blot	5'-TTACAGTCAAATCCCTTCTCGTCC-3'
mtDNA probe R	For southern blot	5'-GGATGAGGCAGGAATCAAAGACAG-3'

Table S2. List of antibodies used in western blotting and Immunofluorescence (IF) experiments.

Protein	Company	Reference	Application	Dilution
MPPB	ptglab	16064-1-AP	Western Blot	1/1000
Lamin B	abcam	ab20396	Western Blot	1/1000
FLAG	SIGMA	F1804	Western Blot and IF	1/2000
Tubulin α	Abgent	AJ1034a	Western Blot	1/1000
hOGG1-1	abcam	ab124741	Western Blot	1/10,000
TOMM22	abcam	ab10436	Western Blot	1/1000
TFAM	abcam	ab155240	Western Blot and IF	1/2000
TOM20	Santa Cruz	sc-11415	Western Blot	1/2000
TIM23	SIGMA	SAB1100941	Western Blot	1/2000
SDHA	abcam	ab14715	Western Blot	1/2000
ETFB	Proteintech	17925-1-AP	Western Blot	1/1000
GARS	abcam	ab42905	Western Blot	1/1000
CS	Proteintech	16131-1-AP	Western Blot	1/1000
CENPF	abcam	Ab5	IF	1:500

Legend to the Figures

Figure 1. αOGG1 is present in both nuclear and mitochondrial compartments. A) Nuclear and mitochondrial fractions were prepared from U2OS cells and analyzed by western blot using an antibody against alpha-OGG1 Antibodies directed against Lamin B and MPPB were used as markers for the nuclear and mitochondrial extracts respectively. **B)** Nuclear and mitochondrial fractions were prepared from U2OS cells expressing OGG1-Flag and analyzed by western blot as in panel A. **C)** U2OS cells transiently transfected with the construct expressing α-OGG1-Flag were analyzed by Immunofluorescence using an antibody against the FLAG epitope (green). Mitotracker Red was used to stain the mitochondrial network (magenta). DAPI was used to stain nuclear DNA (blue). Scale bars, 5μm. **D)** Mitochondria purified from U2OS cells were incubated with different concentrations of Proteinase K. When indicated, mitochondria were exposed to 1% of Triton prior to Proteinase K treatment. Extracts were analyzed by western blot. **E)** Trypsin sequential digestion assays were performed on purified mitochondria from HEK cells. Where indicated, mitochondria were pre-incubated with digitonin (200 or 500 mg/ml) or exposed to hypotonic shock as described in material and methods. **F)** Crude mitochondrial extracts were extracted with increasing concentration of NaCl and insoluble (P) and soluble (S) fraction were isolated and analyzed by western blot.

Figure 2. α-OGG1 is associated with mtDNA in mitochondrial nucleoids. A) Confocal microscopy images of U2OS cells transfected with α-OGG1-FLAG and stained with an antibody against FLAG (red). Mitochondrial DNA is stained with picogreen (green) and the mitochondrial network with MitoTracker Deep Red (magenta). Pearson coefficient (picogreen / OGG1-FLAG) = 0,75, calculated from 8 cells (approximately 1000 nucleoids). Scale bars, 5 μm (2 μm for the insets). **B)** Confocal microscopy images of U2OS cells transfected with α-OGG1-FLAG and MTS-Turquoise2 and stained with antibodies against FLAG (green) and TFAM (red). MTS-Turquoise2 (cyan) was used to label mitochondrial network. Pearson coefficient (TFAM and OGG1-FLAG) = 0,8, calculated as in A. Scale bars, 5 μm (2 μm for the insets) **C)** 3D-SIM was used to visualize α-OGG1-FLAG (green), and TFAM (blue) in the mitochondrial network stained with Mitotracker red (red). Scale bars, 2 μm. **D)** Details of single nucleoids imaged with 3D-SIM. Scale bar, 0,5 μm. **E)** Iodixanol gradient fractions of Mitochondria isolated from HEK cells were analyzed by southern blot using a probe against mitochondrial DNA (upper panel) and western blots using antibodies against TFAM, GARS and α-OGG1. Fractions 1-4 were blank in all cases and are not presented.

Figure 3. α-OGG1 mitochondria-targeting signal (MTS) and nuclear localization signal (NLS) are functional and determine the subcellular localization of the protein. A) Alignment of the N-terminal sequences of OGG1 from human (α-OGG1 isoform), mouse and yeast showing the position of two AUG in frame both human and mouse. The sequence of the MTS is indicated. **B)** Prediction for mitochondrial import calculated with different softwares considering initiation of translation at the first or the second AUG for human and mouse OGG1 proteins. **C)** schematic representation of the WT α-OGG1 or truncations of the

MTS (ΔMTS; initiation of translation at AUG2) or the NLS (ΔNLS) that were fused to the FLAG epitope. **D)** The subcellular localization of different proteins was analyzed by confocal microscopy using antibodies against the FLAG (green). Nuclear DNA is stained with DAPI (blue) and the mitochondrial network with MitoTracker Red (red). **E)** Percentage of cells with a detectable α-OGG1 staining in the mitochondria were quantified. 350 cells were counted for each construct and the experiment was repeated three times. Scale bars, 5 μm and 2 μm in the insets.

Figure 4. Mitochondrial localization of OGG1 is not dependent on the cell cycle phase or mtDNA replication. A) α-OGG1-FLAG was visualized using an anti-FLAG (green), and mitochondrial network was stained with MTS-Turquoise2 (cyan). Cell cycle phases were discriminated by using incorporation of EdU (labels S phase; purple) and an antibody against CENPF (labels G2 phase; Red). The cells negative for both EdU and CENPF are the cells in G1. Scale bar: 5 μm. Higher magnification images of the boxed regions, are presented for the merge MTS-Turquoise and OGG1-FLAG, scale bar: 2 μm. **B)** The percentage of cells with detectable α-OGG1 in mitochondria were determined in the different cell cycle phases. Approximately 500 transfected cells were analyzed from two independent experiments. **C)** Replicating mtDNA was labelled by incorporation of EdU (purple), nucleoids visualised with an antibody against TFAM (red) and α-OGG1-FLAG stained using an anti-FLAG (green). Mitochondrial network was stained with MTS-Turquoise2. Filled and broken arrows indicate replicating and non-replicating nucleoids, respectively. The association of α-OGG1 with nucleoids could be detected in both conditions. Scale bar: 2 μm. **D)** TFAM was used as a marker for nucleoids and the % of nucleoids with a positive signal for α-OGG1-FLAG was determined in both replicating (EdU positive) and non replicating (EdU negative) populations. More than 500 nucleoids were analyzed from 4 cells.

Figure 5. Menadione treatment induces mitochondrial dysfunction in in OGG1-deficient cells. A) U2OS cells were transfected with a siRNA against OGG1 or against a control sequence. 72 hours after transfection, protein extracts were prepared and analyzed by Western Blot using antibodies against α-OGG1. **B)** Effect of Menadione-treatment on the level of mitochondrial superoxide, as detected with the fluorigenic substrate MitoSOX. MitoSOX fluorescence distributions were measured for U2OS siControl (top panel) and U2OS siOGG1 (bottom panel) cell lines, in the absence (grey) or presence (red) of 50 μM Menadione. Probability binning distribution difference analysis was used to quantify the effect of Menadione treatment. Chi-squared based T(X) metrics were calculated for Menadione treated samples as compared to their untreated counterparts, and are indicated in each panel. Results are representative of several independent experiments. **D)** Effect of Menadione-treatment on mitochondrial membrane potential and mitochondrial mass, as detected with TMRE and MitoTracker Green, respectively. TMRE and MitoTracker Green fluorescence was measured for U2OS siControl (top panels) and U2OS siOGG1 (bottom panels) cell lines, in the absence (left panels) or presence (right panels) of 50 μM Menadione. **E)** TMRE and MitoTracker Green fluorescence distributions were plotted as univariate histograms for U2OS siControl (top panels) and

U2OS siOGG1 (bottom panels) cell lines, in the absence (grey) or presence (red) of 50 μM Menadione. Probability binning distribution difference analysis was used to quantify the effect of Menadione treatment on mitochondrial membrane potential. Chi-squared based T(X) metrics were calculated for Menadione treated samples as compared to their untreated counterparts, and are indicated in each panel. Results are representative of several independent experiments. **F)** Living cells transfected with siControl or siOGG1 and stained with MitoTracker green (green) and TMRE (red) were imaged on confocal microscopy. Representative images obtained at different times after exposure to 50 μM menadione for 1 hour are shown. Scale bar, 5 μm.

Figure 6. Mitochondrial dysfunction of OGG1-deficient cells can be complemented with the WT form of α-OGG1 but not with the α-OGG1(ΔMTS) mutant. A) 8-oxoG glycosylase activity was measured in whole cell extracts purified from HeLa cells transiently transfected with plasmids encoding for the WT version of α-OGG1-FLAG or the deletion mutant α-OGG1(ΔMTS)-FLAG. **B)** Western blots on extracts from U2OS cell lines expressing either α-OGG1-FLAG or α-OGG1(ΔMTS)-FLAG in which silent mutations have been introduced into the sequence targeted by the siRNA. Protein levels are not affected by the transfection with siRNA against OGG1 resulting in the silencing of the endogenous protein. **C)** wild type U2OS or cells stably expressing α-OGG1(WT)-FLAG or α-OGG1(ΔMTS)-FLAG were transfected with siRNA against OGG1 72 hours before being exposed to menadione. Mitochondrial ROS production from NT and treated cells was measured in a plate reader using the superoxide indicator MitoSOX Red. Values correspond to the ratio MitoSOX / Hoechst signals. **D)** The same experimental design as in C was used to evaluate mitochondrial membrane potential using TMRE as a probe. Mitotracker Green was used as a marker of mitochondrial mass and the results displayed as a ratio TMRE/Mitotracker Green. For both C and D measurements were performed continuously over a period of 90 minutes after Menadione exposure and the values obtained at 60 minutes are displayed in the graph.

Figure 7. Overexpression of the WT form of α-OGG1 but not the α-OGG1(ΔMTS) or α-OGG1(K249Q) mutants protects mitochondria from Menadione-induced fragmentation. A) U2OS cells transiently expressing different variants of α-OGG1-FLAG, were exposed or not (NT) to Menadione. Transfected cells were stained using antibodies against FLAG (red). The mitochondrial network was stained with Mitotracker Red (purple). Mitochondrial morphology was visualized by confocal microscopy. Only images corresponding to cells transfected with the WT form of α-OGG1 are presented. **B)** Percentage of cells expressing the WT or the different mutants of α-OGG1 (ΔMTS and K249Q) presenting a fragmented mitochondrial network. At least 50 cells were counted. Bars indicate the Mean with SD from three independent experiments. Statistical significance between the different populations was evaluated with Tukey HSD test, $p<0,0001$. **C)** Binarized images were obtained from the mitochondrial red staining. Representative cells expressing each of the α-OGG1-FLAG variants, exposed or not to Menadione, are presented. **D)** After image segmentation, mitochondrial morphology parameters Aspect ratio (AR) and form factor (FF) were determined for each

mitochondria. Dots represents the values for non-transfected cells (black) and for cells overexpressing the WT α-OGG1-FLAG (grey). More than 2000 mitochondria from 8 independent cells treated with menadione are displayed for each population. **E)** Frequency distribution analysis of single mitochondria according to FF **(E)** and AR **(F)** morphological parameters. The analysis was performed for at least 2000 single mitochondria from 8 cells expressing each of the variants. Images were acquired from two independent experiments. Bars indicate Mean +/- SD. Statistical significance between the different populations for the different bins was evaluated with Tukey HSD test, p<0,0001. Scale bars, 5 μm.

Supplementary Figure 1. Conservation of uAUG in the 5' UTR region of α-OGG1. A) First exons containing full or nearly full 5'UTR sequences from vertebrate OGG1 sequences available in Ensembl were multialigned with ClustalW2 (www.ebi.ac.uk/Tools/msa/clustalw2). The two regions containing the starting codons AUG1 and AUG2 are shown. **B)** The degree of conservation and strength of Kozak sequence was investigated using WebLogo (http://weblogo.berkeley.edu/logo.cgi). Sequence logo was calculated for the heptanucleotide surrounding the AUG triplets from position -3 to +4. AUG1 has a G in position -3 in some species but is still fairly leaky. A stronger Kozak sequence was find for AUG2, due to an A in -3 position and a G in +1 position.

Supplementary Figure 2. Subcellular localization of the α-OGG1(WT) and of the mutant α-OGG1(K249Q). Mitotracker RED is used to stain mitochondrial network (red) and OGG1-FLAG is visualized with an antibody anti-FLAG (green). Scale bar, 5 μm and 2 μm in the insets.

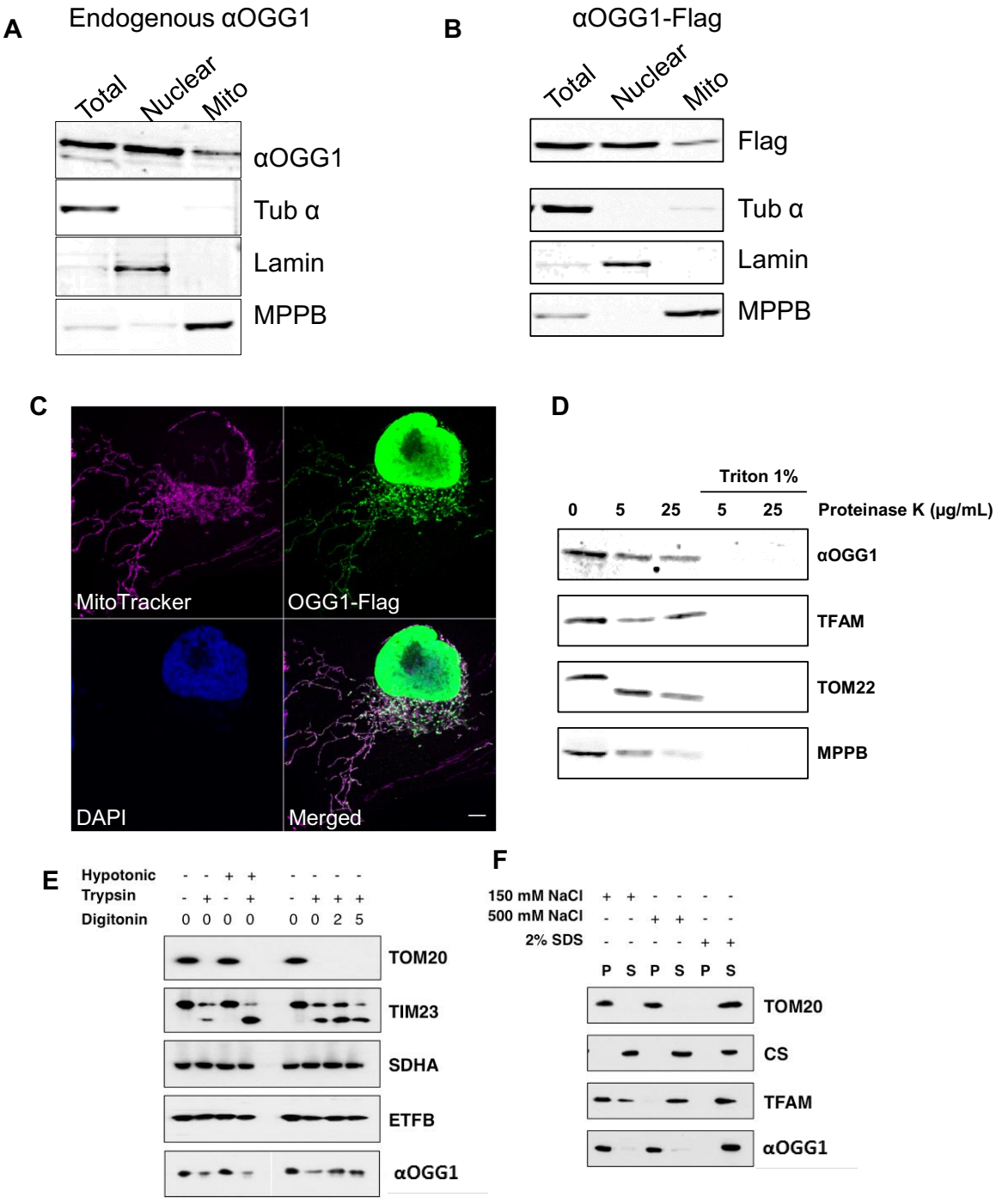
A
Endogenous αOGG1
Total
Nuclear
Mito
αOGG1
Tub α
Lamin
MPPB
B
αOGG1-Flag
Total
Nuclear
Mito
Flag
Tub α
Lamin
MPPB
C
MitoTracker
OGG1-Flag
DAPI
Merged
D
Triton 1%
0 5 25 5 25
Proteinase K (μg/mL)
αOGG1
TFAM
TOM22
MPPB
E
Hypotonic - - + + - - - -
Trypsin - + - + - + + +
Digitonin 0 0 0 0 0 0 2 5
TOM20
TIM23
SDHA
ETFB
αOGG1
F
150 mM NaCl + + - - - -
500 mM NaCl - - + + - -
2% SDS - - - - + +
P S P S P S
TOM20
CS
TFAM
αOGG1

Figure 1

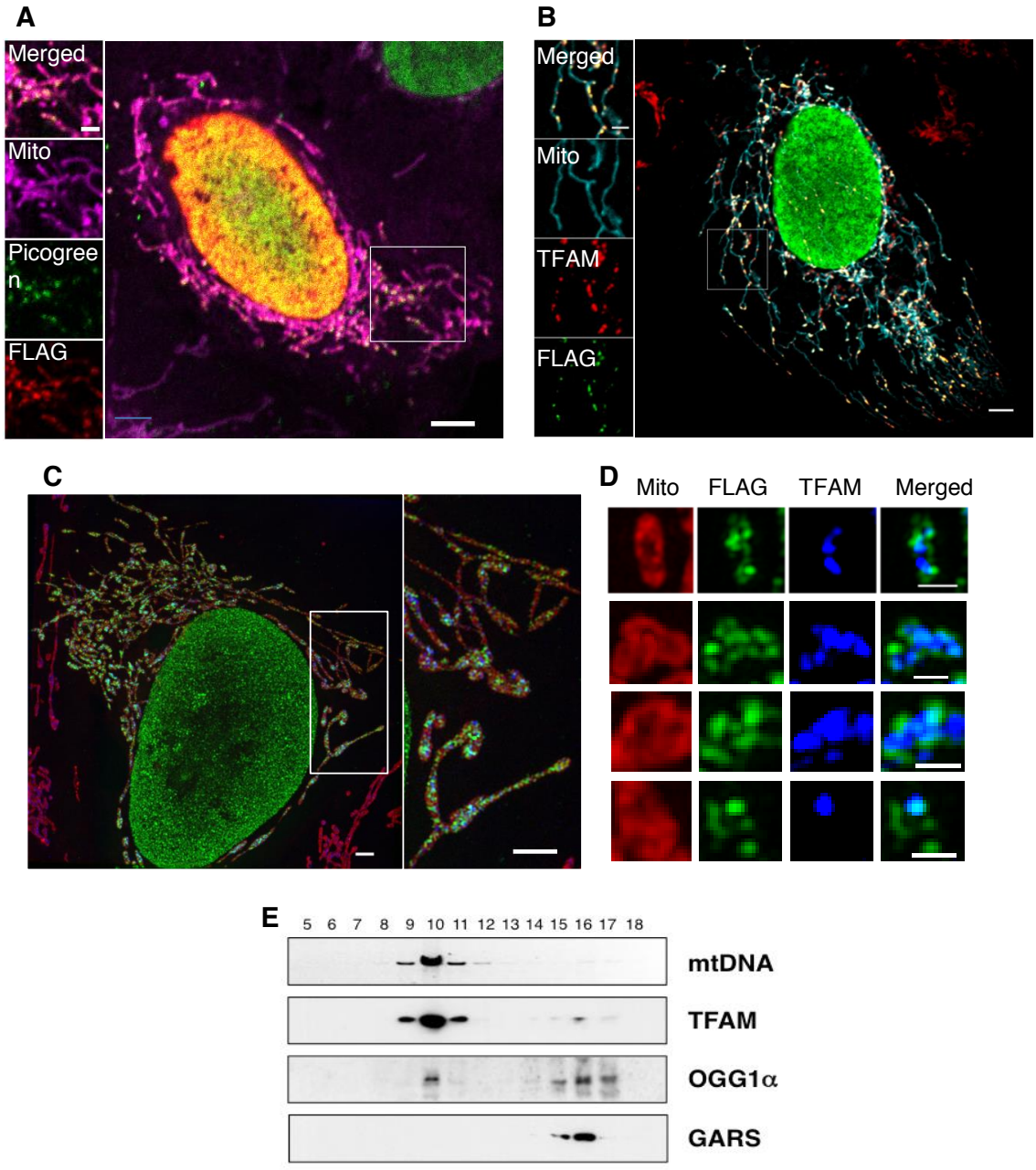

Figure 2

997

998

A

```
H. Sapiens          1   MPARALLPRRMGHRTLASTPALWASIPCPRSEL   33
M. Musculus         1   MLFRSWLPSSMRHRTLSSSPALWASIPCPRSEL   33
S. cerevisiae       1   ----------MSYKFGKLAINKSEL           15
                            MTS
```

B

		Probability of mitochondrial import			
OGG1		MITOPROT	PREDOTAR	PSORTII	TARGETP
Human. 1a	AUG1	0,89	0,81	0,7	0,88
	AUG2	0,3	0,33	0,3	0,61
Mouse	AUG1	0,9	0,8	0,7	0,9
	AUG2	0,53	0,31	0,43	0,7

C

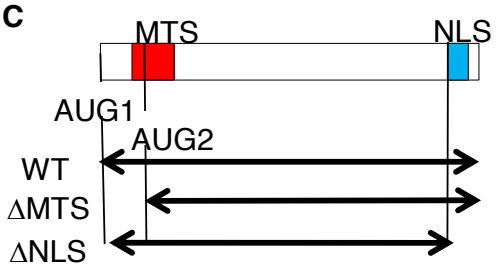

D

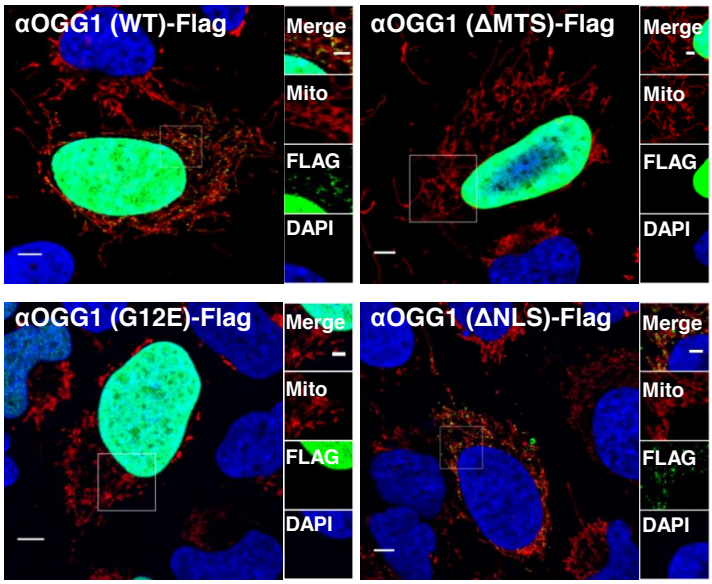

E

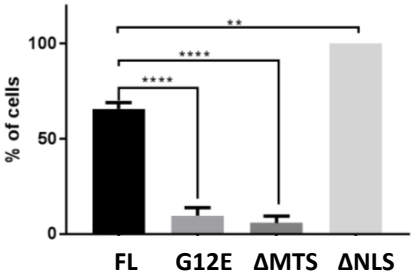

Figure 3

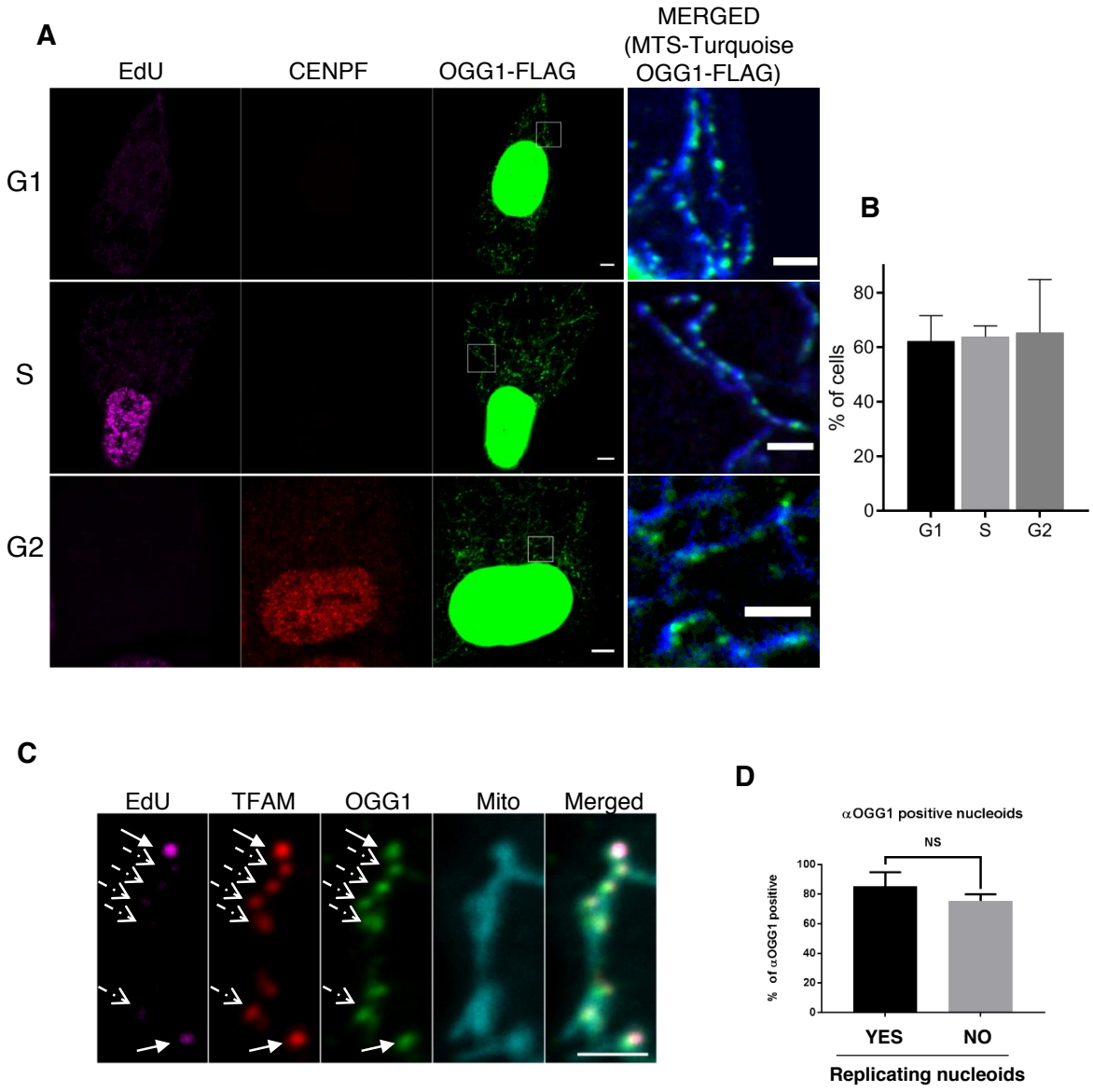

Figure 4

1001

1002

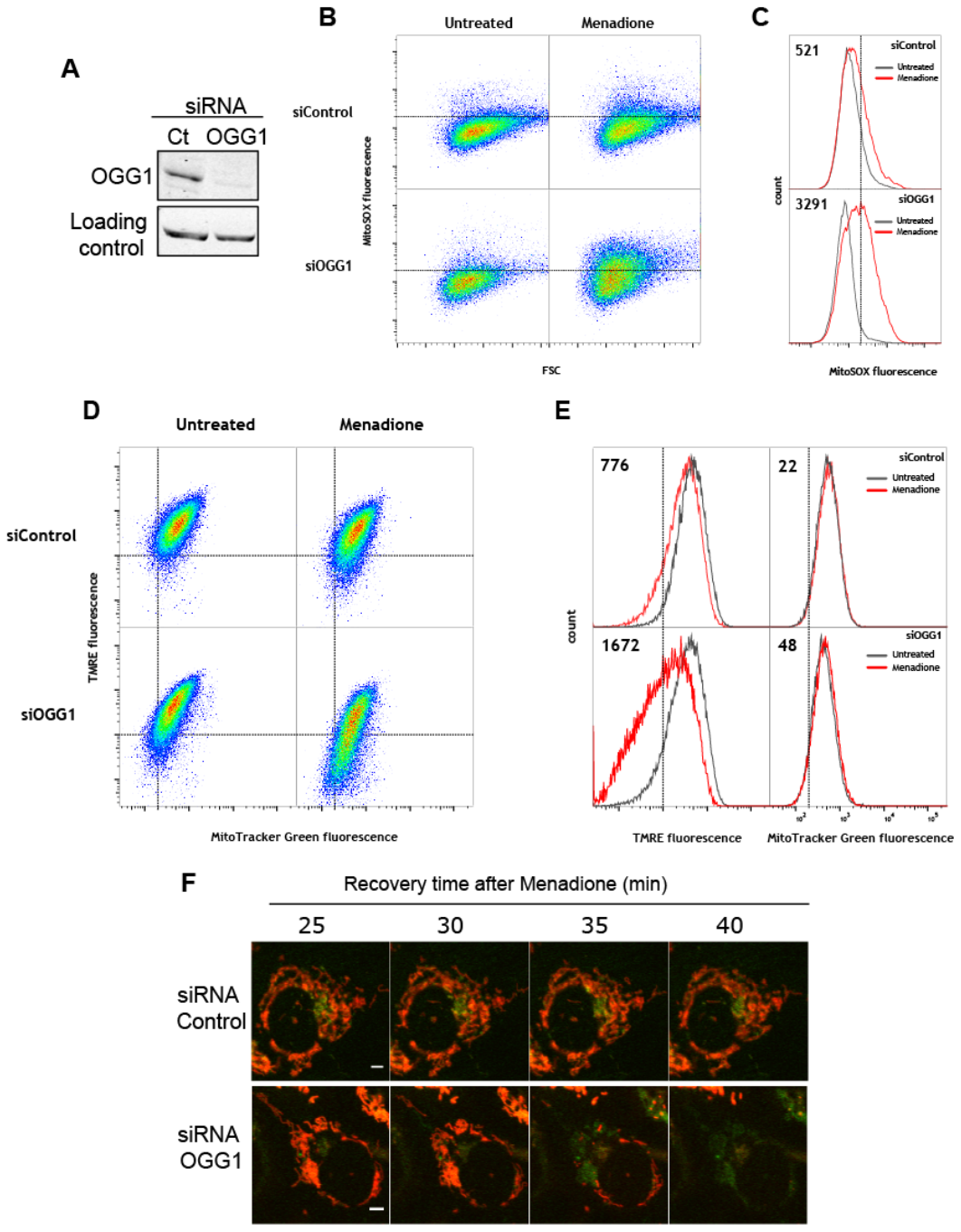

Figure 5

1003

1004

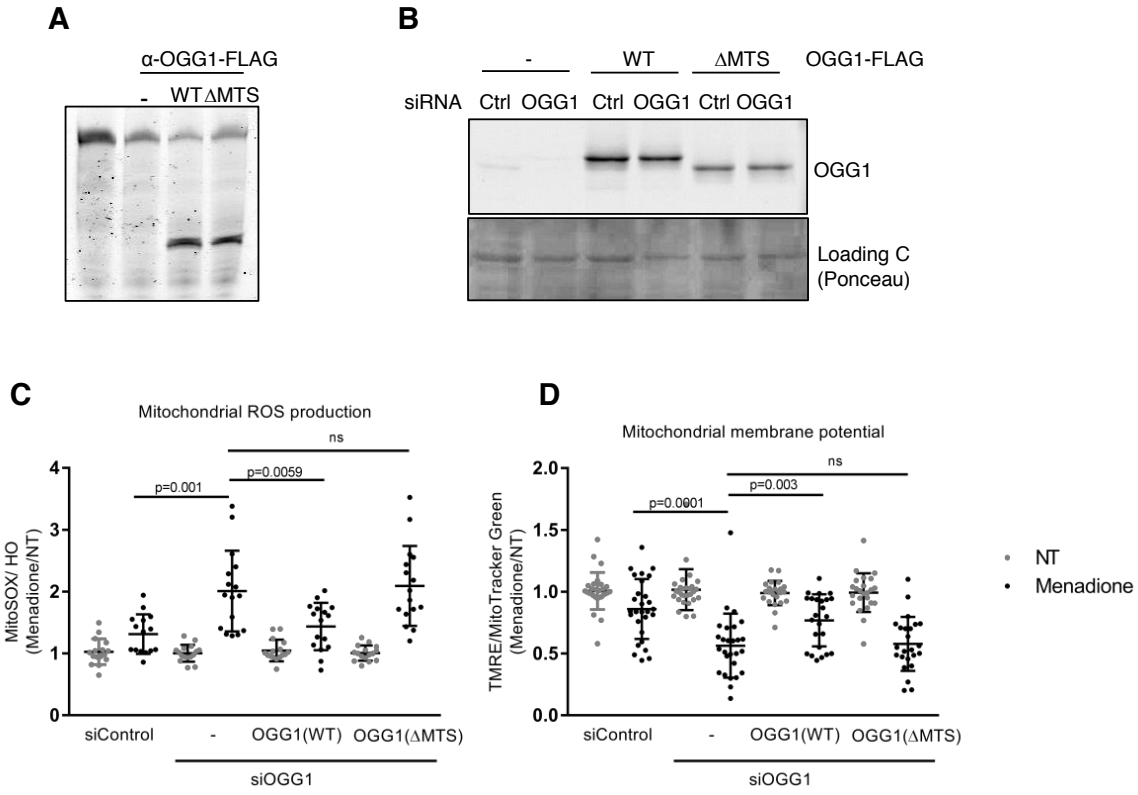
A
α-OGG1-FLAG
- WTΔMTS
B
- WT ΔMTS OGG1-FLAG
siRNA Ctrl OGG1 Ctrl OGG1 Ctrl OGG1
OGG1
Loading C
(Ponceau)
C
Mitochondrial ROS production
MitoSOX/ HO
(Menadione/NT)
p=0.001
p=0.0059
ns
siControl - OGG1(WT) OGG1(ΔMTS)
siOGG1
D
Mitochondrial membrane potential
TMRE/MitoTracker Green
(Menadione/NT)
p=0.0001
p=0.003
ns
siControl - OGG1(WT) OGG1(ΔMTS)
siOGG1
NT
Menadione

Figure 6

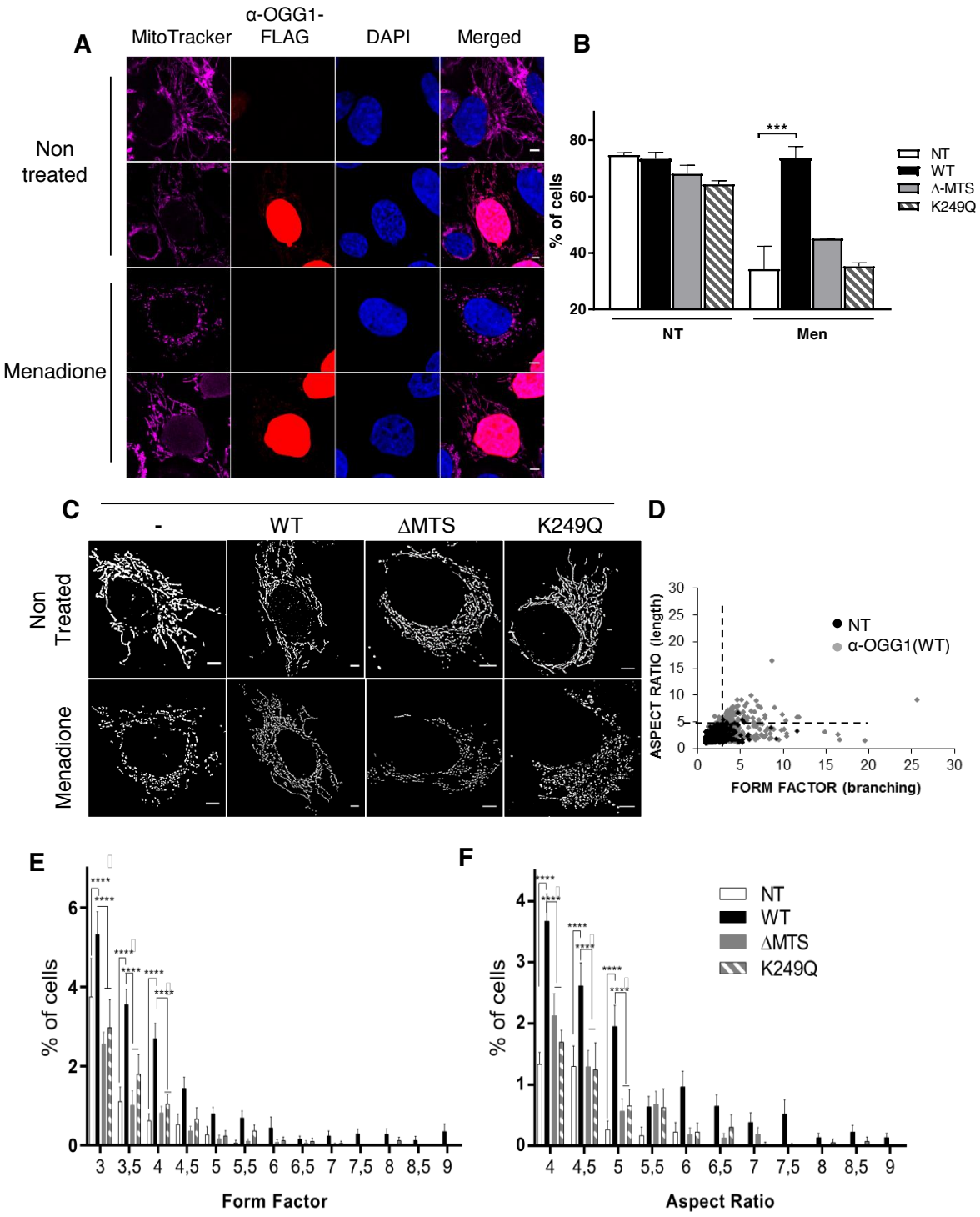
A
MitoTracker
α-OGG1-FLAG
DAPI
Merged
Non treated
Menadione
B
% of cells
***
NT
Men
NT
WT
Δ-MTS
K249Q
C
-
WT
ΔMTS
K249Q
Non Treated
Menadione
D
ASPECT RATIO (length)
FORM FACTOR (branching)
NT
α-OGG1(WT)
E
% of cells
Form Factor
F
% of cells
Aspect Ratio
NT
WT
ΔMTS
K249Q

Figure 7

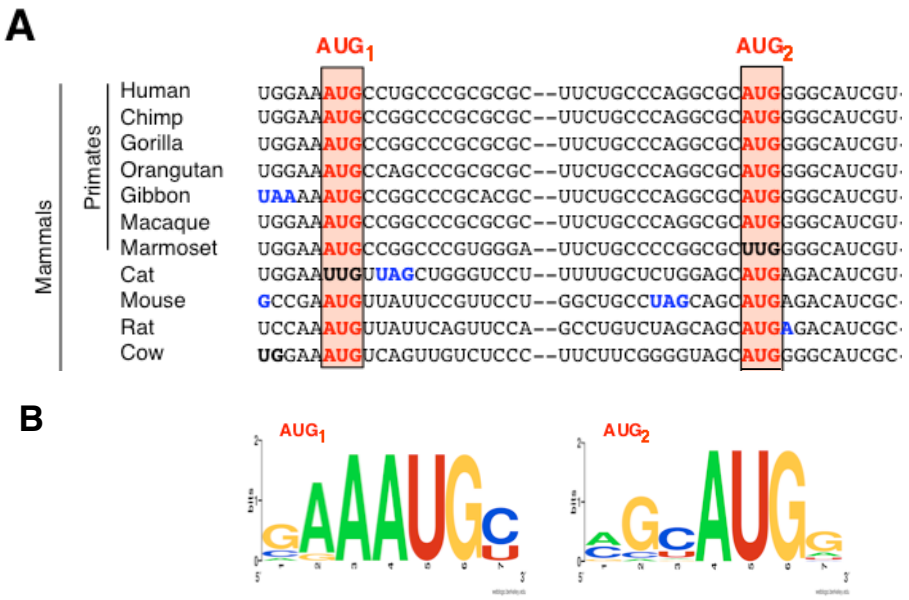

Supplementary Figure 1.

1009

1010

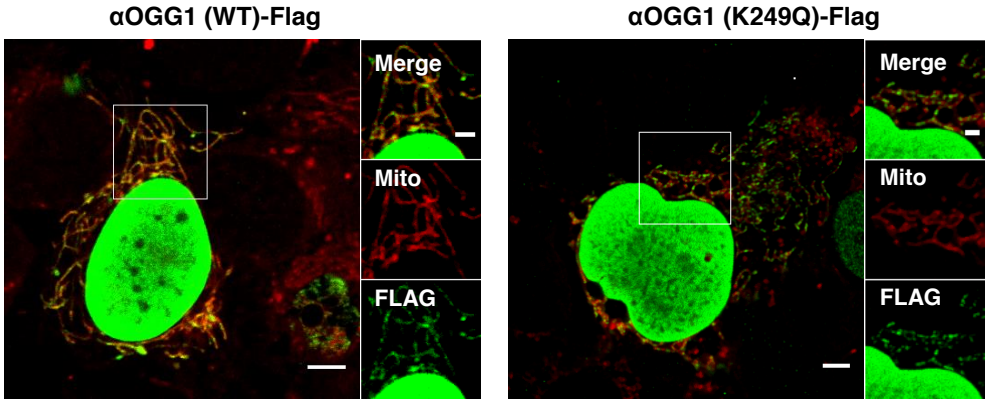

Supplementary Figure 1